ISCA1 Deficiency Induces Iron Metabolism Disorder and Myocardial Oncosis in Rat

Yahao Ling
ILAS: Chinese Academy of Medical Sciences Institute of Laboratory Animal Sciences
Xinlan Yang
ILAS: Chinese Academy of Medical Sciences Institute of Laboratory Animal Sciences
Xu Zhang
ILAS: Chinese Academy of Medical Sciences Institute of Laboratory Animal Sciences
Feifei Guan
ILAS: Chinese Academy of Medical Sciences Institute of Laboratory Animal Sciences
Xiaolong Qi
ILAS: Chinese Academy of Medical Sciences Institute of Laboratory Animal Sciences
Wei Dong
ILAS: Chinese Academy of Medical Sciences Institute of Laboratory Animal Sciences
Mengdi Liu
ILAS: Chinese Academy of Medical Sciences Institute of Laboratory Animal Sciences
Jiaxin Ma
ILAS: Chinese Academy of Medical Sciences Institute of Laboratory Animal Sciences
Xiaoyu Jiang
ILAS: Chinese Academy of Medical Sciences Institute of Laboratory Animal Sciences
Kai Gao
ILAS: Chinese Academy of Medical Sciences Institute of Laboratory Animal Sciences
Jing Li
ILAS: Chinese Academy of Medical Sciences Institute of Laboratory Animal Sciences
Wei Chen
ILAS: Chinese Academy of Medical Sciences Institute of Laboratory Animal Sciences
Shan Gao
ILAS: Chinese Academy of Medical Sciences Institute of Laboratory Animal Sciences
Xiang Gao
ILAS: Chinese Academy of Medical Sciences Institute of Laboratory Animal Sciences
Shuo Pan
ILAS: Chinese Academy of Medical Sciences Institute of Laboratory Animal Sciences
Yuanwu Ma
ILAS: Chinese Academy of Medical Sciences Institute of Laboratory Animal Sciences
Jizheng Wang

Chinese Academy of Medical Sciences & Peking Union Medical College Fuwai Hospital

Dan Lu

ILAS: Chinese Academy of Medical Sciences Institute of Laboratory Animal Sciences

lianfeng zhang (zhanglf@cnilas.org)

Chinese Academy of Medical Sciences & Peking Union Medical College Institute of Laboratory Animal Science https://orcid.org/0000-0002-5774-2924

Research Article

Keywords: ISCA1, heart failure, oncosis, STEAP3, iron ion metabolism.

Posted Date: July 13th, 2021

DOI: https://doi.org/10.21203/rs.3.rs-648138/v1

Title: ISCA1 deficiency induces iron metabolism disorder and myocardial oncosis in rat

Running title: ISCA1 deficiency induces myocardial oncosis in rat

Authors: Yahao Ling[1,4], Xinlan Yang[1,4], Xu Zhang[2], Feifei Guan[2], Xiaolong Qi[2], Wei Dong[1], Mengdi Liu[2], Jiaxin Ma[2], Xiaoyu Jiang[2], Kai Gao[1], Jing Li[2], Wei Chen[1], Shan Gao[1], Xiang Gao[1], Shuo Pan[2], Yuanwu Ma[1], Jizheng Wang[3], Dan Lu[2*], Lianfeng Zhang[1*]

1. Key Laboratory of Human Disease Comparative Medicine, National Health Commission of China (NHC), Institute of Laboratory Animal Science, Peking Union Medical College, Chinese Academy of Medical Sciences, China.

2. Beijing Engineering Research Center for Experimental Animal Models of Human Diseases, Institute of Laboratory Animal Science, Peking Union Medical College, Chinese Academy of Medical Sciences, China.

3. State Key Laboratory of Cardiovascular Disease, Fuwai Hospital, National Center for Cardiovascular Disease, Chinese Academy of Medical Sciences and Peking Union Medical College, China.

4. These authors contributed equally to this work.

***Corresponding author:**

Lian-Feng Zhang, Ph.D. and Dan Lu, Ph.D.

Building 5, PanjiayuanNanli, Chaoyang District, Beijing 100021 P. R. China.

E-mail: zhanglf@cnilas.org or lvd@cnilas.org; Phone and Fax: 86-010-67776394.

Abstract

The effects of multiple mitochondrial dysfunction (MMD) on heart, a highly mitochondria-dependent tissue, is still unclear. This study was the first to verify the effect of ISCA1 gene deficiency, which has been shown to cause multiple mitochondrial dysfunction syndromes type 5 (MMDS5), on cardiac development *in vivo*, that is cardiomyocytes suffer from energy shortage due to abnormal metabolism of iron ion, which leads to oncosis and eventually HF and body death. Subsequently, we determine a new interacting molecule for ISCA1, six-transmembrane epithelial antigen of prostate 3 (STEAP3), which acts as a reductase in the reduction of Fe^{3+} to Fe^{2+}. Forward and reverse validation experiments demonstrated that STEAP3 plays an important role in iron metabolism and energy generation impairment induced by ISCA1 deficiency. This result provides theoretical basis for understanding of MMDS pathogenesis, especially on heart development and the pathological process of heart diseases, and finally provides new clues for searching of clinical therapeutic targets.

Key Words: ISCA1; heart failure; oncosis; STEAP3; iron ion metabolism.

Introduction

Mitochondrial metabolic pathways impaired and then interfere with energy production, which have been defined as multiple mitochondrial dysfunction syndromes (MMDS). MMDS can lead to complex damage of mitochondrial structure and function, and weaken the function of mitochondrial respiratory complex, which then lead to the serious damage of various metabolic pathways, including infantile-onset mitochondrial encephalopathy, myopathy and early death[1, 38]. Previous study showed that MMDS refers not only to cerebral abnormalities but also to multiorgan disease, including the eyes, endocrine organs, heart, lungs and the gastrointestinal tract[3, 6].

The lack of energy production caused by gene mutation is considered as the pathogenic basis of MMDS. Current research has found that multiple diseases are associated with the biosynthetic pathway of mitochondrial iron-sulfur clusters (ISC). Mutations in genes involved in synthesis of ISC may severely impair diverse mitochondrial metabolic pathways and interfere with energy production[2, 6, 27], including NFU1, BOLA3, IBA57, ISCA2, ISCA1 and PMPCB[2, 3, 6, 27, 35, 43]. And according to genes involved in this disease, MMDS include six types, that is MMDS1 (NFU1), MMDS2 (BOLA3), MMDS3 (IBA57), MMDS4 (ISCA2), MMDS5 (ISCA1) and MMDS6 (PMPCB).

Abnormal muscle or heart development was also observed in MMDS2，MMDS3，MMDS5 and MMDS6 types, in addition to neurodegenerative changes. BOLA3 deficiency patient developed cardiomyopathy[28]. IBA57 patient develop severe myopathy[5]. The mutation in the ISCA1 gene results in spasticity with exaggerated deep tendon reflexes[35, 36, 41]. And one feature from PMPCB patient was dystonia[43].

It is widely accepted that the adult heart, just like brain, is a highly energy-demanding tissue. Mitochondrial oxidative phosphorylation is responsible for nearly all of the ATP production (>95%) in adult mammalian hearts[24, 40]. Therefore, the normal function of mitochondria is of great importance to the cardiac pump function. However, there are few studies on the relationship between MMDS and cardiac development, and the effects of ISC-related gene mutation or abnormal expression on cardiac development is still unclear. The study about MMDS induced by ISC synthesis related gene deletion on cardiac development, are helpful to understand the effects of MMDS on important organs except brain and nervous system, as well as its possible pathogenic mechanism.

ISCA1 belongs to the A-type ISC proteins and functions as a late-acting component of the mitochondrial [4Fe–4S] clusters assembly machinery in key metabolic and respiratory enzymes[33]. ISCA1-related multiple mitochondrial dysfunctions syndrome (ISCA1-MMDS) is a severe neurodegenerative disorder typically characterized by developmental delay, seizures in early infancy, exaggerated deep tendon reflexes and so on[33,

35, 36, 41]. At the same time, our previous study exhibited that the expression of ISCA1 significantly increased in myocardium from patients and animal models with cardiomyopathy. These findings suggested us that the abnormal expression of ISCA1 may affect the development of the heart. However, the effects of ISC-related genes on heart development are still poorly characterized.

Therefore, in this study we first generated an ISCA1 conditional knockout rat using CRISPR-Cas9 technology (referred to as *Isca1* cKO). We then selectively eliminated the ISCA1 in myocardium by crossing *Isca1* cKO rat with our previous established *α myosin heavy chain Cre* (*α-MHC-Cre*) rat. Subsequently, we investigated the effects of ISCA1 deficiency on cardiac development, as well as on the myocardial mitochondrial energy metabolism and its possible molecular mechanism. Taken together, we found that ISCA1 deficiency can induce severe heart failure (HF) and the cardiomyocytes represented as oncosis. Furthermore, we found that ISCA1 interacts with six-transmembrane epithelial antigen of prostate 3 (STEAP3), a member of the oxidoreductase family. We found that ferrous iron (Fe^{2+}) obtained by ISCA1 reduced significantly with STEAP3 knowdown regulated. Meanwhile, we found that the level of ferric iron (Fe^{3+}) and Fe^{2+} undergo different degrees of regulation, and the iron homeostasis suffered a destruction in myocardium with ISCA1 deficiency. Furthermore, impaired formation of Fe/S complex and function of myocardial mitochondrial complex and insufficient energy supply of myocardium, eventually leads to HF and body death.

This paper showed that the effects of MMDS, induced by gene mutation involved in iron-sulfur cluster biosynthesis, on cardiac development, and the possible mechanism of ISCA1 involved in iron metabolism. Our results provide theoretical basis and clues for understanding of MMDS pathogenesis and exploring novel clinical therapeutic targets.

Methods

1. Animals

1.1 Generation of myocardium specific *Isca1* knockout rats

The *Isca1*-floxed rats (referred to as *Isca1* conditional knockout, *Isca1* cKO), were produced using the CRISPR/Cas9 system[23]. In brief, two sgRNAs targeting sites (sgRNA1: GCCTCCTGAGCAAGTGCT; sgRNA2: AGCCCTGAACTCCTTATG) were designed and applied for inserting the *loxP* sites into the intron upstream and downstream of exon 3 (Figure 2A). The newly produced rats were genotyped with target specific primers (Supplemental Table 1). The correct insertion was further confirmed by sequencing. *α-MHC-Cre* transgenic rats were established in our laboratory as previously reported[22, 46]. Animals carrying the *α-MHC-Cre* transgene were identified using PCR analysis of tissue genomic DNA using Cre-specific primers (Supplemental Table 1). The positive transgenic rats would be then maintained through mating with wild type (WT) SD rats.

Myocardium specific *Isca1* knockout rats were generated using the *Cre-lox*P system by crossing *α-MHC-Cre* rats with *Isca1*-floxed rats (*Isca1* cKO). The offspring with genotype of positive *α-MHC-Cre* transgene and $Isca1^{flox/+}$, was called double-positive rats, which were reserved and selected. The double-positive rats were then mating with *Isca1* cKO rats in the second round of hybridization, and offspring with genotype of positive *α-MHC-Cre* transgene and $Isca1^{flox/flox}$ were selected as myocardium specific *Isca1* knockout ($Isca1^{flox/flox}$/*α-MHC-Cre*) rats, and referred to as *Isca1* KO rats in this paper (Figure 2B). The *Isca1* KO rats were used in the following analysis and WT littermates were used as control. In addition, rat information used in this study can be found in our rat database (www.ratresource.com).

The background of rat used in this study was Sprague-Dawley rat. All rats were maintained in standard cages in an Association for Assessment and Accreditation of Laboratory Animal Care (AAALAC) accredited animal facility. All animal experiments were approved by Animal Care and Use Committee of the Institute of Laboratory Animal Science of Peking Union Medical College with the permission No. MYW20002.

1.2 Thoracic aorta constriction (TAC) induced hypertrophic mice model

C57BL6 mice at 8~10 weeks of age were used for TAC operation according to the protocols described previously[11, 20]. In brief, the mice were anesthetized by intraperitoneal administration of tribromoethanol (216 mg/kg body weight). The surgical operation was performed under passive respiration with a ventilator (125~150 times/min, Kent Scientific Torrington, USA). The aorta constriction was performed using a 27-gauge (0.41 mm OD) blunted needle as a calibrator and ligatured with a 6/0 polypropylene. The sham surgery was carried out

exactly the same to TAC without ligating the aorta. Each surgical treatment was completed within 30 min to maintaining constant body temperature at 37℃. The mice would be received 0.9% saline solution intraperitoneally if dehydration occurred. The surviving mice were selected for follow up studies at 4 weeks after the operation.

1.3 Adriamycin (ADR) induced heart failure mice model

C57BL6 mice at 8~10 weeks of age were used for ADR treatment as previous reported[11, 19, 46]. Briefly, ADR was treated with a constant dose of saline intraperitoneally at 4 mg/kg every other day for 2 weeks. The surviving mice would be firstly carried out by echocardiographic studies at 2 weeks after ceasing of administration of ADR and then selected for follow up studies.

2. Human cardiac samples

Study protocol with human samples were approved by the Ethics Committee of Fuwai Hospital of PUMC and following the Declaration of Helsinki. The cardiac samples collected from the interventricular septum of the left ventricle were obtained from 5 patients with obstructive HCM who went through morrow septal myectomy. The normal cardiac samples were acquired from the same cardiac region in 4 healthy donors who died in accidents. None of the donors of normal group had a history of heart disease. The cardiac samples were kept in liquid nitrogen until they were used.

3. Genomic DNA preparation and genotyping

EasyPure® Genomic DNA Kit (China, Trans Gen Biotech, EE101-22) was used to acquire the extraction of Genomic DNA from the tail tissue of 7-day-old rats according to the manufacturer's instructions. The lysis buffer and proteinase K (20 mg/mL) was applied to dissolve the rat tail tissue and incubated in a swing bed at 55 °C for 6~8 hours. Silica-based column specific bound to DNA was used, the tissue lysate was then extracted. The genomic DNA was eluted by adding 150 μL of elution buffer (preheated to 60-70°C before use)[22, 46]. The PCR amplification for genotyping of *Isca1* cKO rats was carried out using program: 95 ℃,15 min; 30 cycles consist of 95 ℃ for 30 s, 59 ℃ for 30 s, and 72 ℃ for 2 min; 72 ℃, 10 min; 4 ℃, indefinite.

4. Survival Analysis

The cumulative percentage mortality of the WT littermate control rats (including *Isca1*$^{+/+}$, *Isca1*$^{flox/+}$ *and* *Isca1*$^{flox/flox}$) and the *Isca1* KO rats (*Isca1*$^{flox/flox}$*/α-MHC-Cre*) was calculated from birth to 10 days of age. The body was autopsied by a pathologist after the death of each rat and pathological changes and morphological alterations of the heart were recorded. The Kaplan–Meier curves were analyzed through comparison with the log-rank test (GraphPad Prism8 software)[20].

5. Echocardiography

The echocardiographic inspection was performed using small animal echocardiography analysis system (Vevo770 and Vevo3100, Canada) as previously described[11, 20]. The parameter of the left ventricular (LV) diameter (LVID) and LV anterior wall (LVAW) at end diastole and end systolic, and LV ejection fraction (LVEF) and LV percent fractional shortening (LVFS) were measured. The mean value of at least three continuous cardiac cycles were recorded.

6. MRI (magnetic resonance imaging)

The rats were anesthetized with 1.5%~2% isofluorane at 6.5 days of age. MRI-compatible system (SA Instruments, Stony Brook, NY, USA) was used to monitor the electrocardiography of rat. The structure and function parameters of the atria and ventricular were detected and analyzed with a varian 7.0T small animal MRI imaging technology (Varian, Palo Alto, CA, USA). The scan parameters were recorded, including TReff: 145.9 ms; TE: 1.29 ms; Flip Angle: 30 deg; thickness: 1 mm; Gap: 0 mm; FOV: 30×30 mm; Matrix: 128×128.

7. Evans blue dye treatment

Evans blue (EB) dye was used to assess the sarcolemmal membrane permeability and structural integrity of myocardial cell as reported previously[15]. 134mg Evans blue dye powder (USA, Sigma-Aldrich, E2129, dye content≥75%) was dissolved in 5mL saline solution formulated as a mixed solution of 2% concentration and filtrated with a 0.22μm filter. The *Isca1* KO rats (1.5-day-old and 5.5-day-old) were injected with EB solution (30mg/kg) through the common carotid artery. All the surviving rats were kept alive for 24 hours and heart tissues were obtained for the following study.

8. Histological Analysis

Cardiac tissues were fixed with 4% formaldehyde, mounted in paraffin and then sectioned (3~4 μm in thickness) using a Tissue-Tek® Sledge microtome (IVS-410, SAKURA, Japan). The sections were stained with hematoxylin and eosin (H&E) and then observed with a light microscope (NanoZoomer S60, C13210, Hamamatsu Photonics, Japan) as previously described[19, 20]. All sections were analyzed using the NDP.view2 image viewing software.

9. Transmission electron microscopy (TEM)

For the analysis of TEM, cardiac tissues were routinely fixed in glutaraldehyde (2.5%) and phosphate buffer (0.1 M, pH 7.4), then fixed in osmium tetroxide buffer (1%) for 1 hr. The sections were examined under a JEM-1230 Transmission electron microscopy after stained with uranyl acetate and lead citrate as described previously[19, 46].

10. Protein extraction and immunoblotting

Total protein lysates were prepared from rat heart tissues or collected cells using protein extraction reagent (USA,

Thermo, 78510) or RIPA buffer (USA, Thermo, 89901) as described previously[19, 32]. Mitochondria/cytosol fractionation kit (UK, Abcam, ab65320) was used for isolation of mitochondrial and cytosolic fractions from cardiac tissues follow the instructions in the manual[39]. Protein concentrations was determined by using a BCA protein assay Kit (USA, Thermo, 23225). Protein extracts were separated by SDS-PAGE and transferred to nitrocellulose membranes. The membranes were incubated at 4℃ overnight with appropriate primary antibodies (ISCA1 (USA, Thermo, PA5-60121); STEAP3 (UK, Abcam, ab151566); TOMM20 (USA, Thermo, PA5-52843); NDUFA9 (UK, Abcam, ab14713); NDUFS3 (UK, Abcam, ab110246); SDHB (UK, Abcam, ab14714); GAPDH (UK, Abcam, ab201822)) and subsequently kept for 1 h at room temperature with the appropriate secondary antibodies. Western blot images were acquisition (Bio-Rad, ChemiDoc XRS+ Gel Imaging System, USA) and quantitatively analyzed with Image J software.

11. Immunofluorescence

Sections of cardiac tissues were performed using a standard pathological procedure as described previously[20]. The sections were dewaxed and rehydrated, and epitopes were unmasked. Then the sections were blocked and incubated with appropriate antibodies (VDAC1 (UK, Abcam, ab235143); Dystrophin (UK, Abcam, ab15277); ISCA1 (USA, Thermo, PA5-60121); STEAP3 (USA, SANTA CRUZ, sc-376327); Wheat Germ Agglutinin Conjugates (USA, Invitrogen, W7024)), respectively, overnight at 4 ℃. After washing with PBS, the sections were incubated with corresponding secondary antibodies for 1h at room temperature. Sections were then counterstained with a fluorescent mounting medium with DAPI (China, ZSGB-BIO, ZLI-95557). Images of sections were captured by a confocal laser scanning microscopy (TCS LSI, Leica, Germany; Pannoramic 250 Flash III and 3D HISTECH, Hungary; TCS SP8 DIVE, Leica, Germany).

12. Cell culture and stable transfected cell line screen

The H9c2 cardiomyocytes were cultured in DMEM medium (USA, Gibco, 11965-092) supplemented with 10% FBS (USA, Gibco, 10099-141C) in an incubator containing 5% CO_2 at 37 °C[11]. Steap3-shRNA or the control-shRNA plasmids (USA, Origene, TL712607) were transfected into H9c2 cardiomyocytes with Lipofectamine 2000 transfection reagent (USA, Invitrogen, 11668-019) in 6 cm plate according to the manufacturer's instructions. The stable transfected clone was selected with culture media containing 1.0 μg/ml puromycin (USA, Sigma-Aldrich, P8833) for 2 weeks. After 2-3 generations under the action of puromycin and the determination of STEAP3 expression, the stable H9c2 cells were used for the following assay.

13. Immunoprecipitation assays

For test of interacting molecular screening, stable H9c2 cell line with ISCA1 (with Flag tag) overexpression was

firstly established, and cells were collected and lysis in ice-cold IP lysis buffer (USA, Pierce, 87787). The lysates were sonicated and centrifuged at 14000g at 4°C for 40 min. The supernatants were incubated with ANTI-FLAG M2 Affinity Gel (USA, Sigma-Aldrich, A220) with gently shaking as indicated for 3 hr at 4°C. The beads were washed three times with ice-cold IP lysis buffer and then heated at 95°C for 5min. The collected supernatants were determinate using western blot. For preparation of immunoprecipitation products against ISCA1 antibody in stable STEAP3-kd cell, the total cell lysates were prepared in IP lysis buffer (0.5 mL per 5×10^6 cells/60 mm^2 dish). 20 μL of ISCA1 antibody (100 μg/mL, USA, SANTA CRUZ, sc-133426) was added with 230 μL IP lysis buffer to prepare antibody working solution. The finally collected supernatants was used for the following ferrous iron measurements.

14. Iron ion assay

The levels of total iron, ferrous iron (Fe^{2+}) and ferric iron (Fe^{3+}) in cardiac tissues were determined by iron assay kit according to the manufacturer's protocols (UK, Abcam, ab83366). The cardiac tissues or collected cells were homogenized in iron assay buffer on ice, then centrifuged (16,000 × g, 10 min) and then the supernatant was collected. 50 μL of samples were used per well in a 96-well plate. Subsequently, 5 μL iron reducer was added to each well, and incubate at 37°C for 30 minutes. Then 100 μL iron probe were added to each sample and incubate at 37°C for 1h away from light. The samples were measured with a micro-plate reader (at 593 nm) according to the colorimetric assay[49]. For cell experiment, the stable STEAP3-Kd cells were collected for immunoprecipitation assay after treating with 100 μM ferric ammonium citrate (FAC, China, Sangon Biotech, A500061) for 24 hrs. The collected lysis was used for iron assay and the method was the same with cardiac tissues as described above.

15. ATP measurement

ATP assay kit (USA, Biovision, K354-100) was used for measurement of myocardial ATP content as previous described[13]. Briefly, 40mg of cardiac tissues from 6.5-day-old *Isca1* KO rats or collected cells (7×10^6 cells) were homogenized in 400 μl of ATP assay buffer and deproteinized by using deproteinizing sample preparation kit (UK, Abcam, ab204708). The standard curve was prepared according to the colorimetric assay and the absorbancewas measured in a micro-plate reader at 570 nm.

16. Measurement of mitochondrial respiratory complex enzyme activity

Activities of mitochondrial respiratory complex I, II, IV were analyzed using enzyme assay kits (UK, Abcam, ab109721, ab109908, ab109911) according to the manufacturer's protocols as previous described[50]. In brief, 30mg of heart tissues from 6.5-day-old *Isca1* KO rats were homogenized for harvesting the extracts of

mitochondria. The microplate wells were precoated with specific capture antibodies for measuring complex I, II, IV activity. Then the samples were added to microplate wells to capture enzyme and incubate. Enzyme activities were measured by colorimetric method.

17. RNA extraction and real-time PCR

Total RNA was extracted from the freshly harvested heart tissues or collected cells by using TRIzol reagent (USA, Ambion, 15596018) as previously reported[19-21]. According to the manufacturer's instructions (Japan, TaKaRa, RRO47A), 1 μg of total RNA was used to synthesize first-strand cDNA using Superscript III reverse transcriptase. The nppa and nppb mRNA levels were normalized to GAPDH. The PCR reactions were amplified and analyzed by using the Real-Time PCR System (QuantStudio 3, Thermo, USA). Primers sequences were showed in online supplemental table 1.

18. Calcein-AM/Propidium Iodide Cell-Survival Assay

The cell viability of H9c2 cells were evaluated by Calcein-AM/PI Double Staining Kit (Japan, Dojindo, C542) according to the manufacturer's instructions[26]. Briefly, 4μl Calcein-AM storage solution and 4μl Propidium Iodide (PI) storage solution were added into 4 ml PBS to become staining working solution (Calcein-AM: 1 μmol/L and PI: 1.5 μmol/L). Removed the cell culture medium and washed the cells with PBS twice. Then the staining working solution was added to the cells and cultured at 37 °C for 5 min. The live cells were stained with calcein AM (green fluorescence) and dead cells were stained with PI (red fluorescence) and observed under a fluorescence microscope (AF 6000, Leica, Germany). The live and dead cells were quantified using Image J software.

19. Statistical analysis

The experimental data are expressed as means ± SD and analyzed with unpaired two-tailed Student's t-tests for two groups or one-way analysis of variance (ANOVA, with Tukey correction) for multiple groups. GraphPad Prism8 software is used for statistical analysis and significance is considered as $P<0.05$.

Results

1. ISCA1 is induced under cardiomyopathy and heart failure and expressed in myocardial mitochondria

We first verified the expression characteristics of ISCA1 under pathology. We found that ISCA1 increased significantly in heart tissues from adriamycin (ADR) induced dilated cardiomyopathy and pressure overload induced (TAC treatment) heart failure (HF) mice (Figure 1A and 1B, n=4 mice per group, P<0.001 *versus* respectively control). Immediately after, we examined ISCA1 expression in HCM patients and healthy heart donors, and ISCA1 expression similarly increased significantly under HCM in human heart tissues (Figures 1C and 1D, n=4 in normal group and n=5 in HCM group, P<0.001 *versus* normal).

To identify the location of expressed ISCA1 protein in cardiomyocytes, we stained heart tissue sections from WT rat at 2 weeks of age. Immunofluorescence analysis revealed that ISCA1 localized primarily in the mitochondria of myocardium, as colocation with the mitochondrial marker of VDAC1, and with small quantities in the cytoplasm (Figure 1E).

The abnormally elevated expression of ISCA1 under pathological states reminder us that this gene may be involved in heart development and pathological process of heart diseases.

2. Myocardial specific ISCA1 deficiency induces severe HF in rats

To investigate the effects of ISCA1 on organ development, we first established ISCA1 knockout rats by replacing the exon 1 of ISCA1 gene with the *mCherry-Cre* fusion gene using CRISPR-Cas9 technology in our lab as previously reported[48]. We found that knockout homozygous rats (*Isca1 mCherry-Cre*$^{-/-}$) cannot be available in the pups born, which arrested fetal development at E8.5[48].

Thus, to further explore how ISCA1 shapes heart morphology and function *in vivo*, we first established *Isca1* conditional knockout (*Isca1* cKO) rat in this study (Figure 2A), and selectively eliminated ISCA1 from the *α-MHC* rat genome by crossing *Isca1* cKO rats with the *α-MHC-Cre* rats (Figure 2B). After two generation of cross mating, homozygous rat with myocardial tissue specific knockout of ISCA1 was obtained from the offspring, referred as *Isca1*-KO (*Isca1*$^{flox/flox}$*/α-MHC-Cre*). KO rat and its WT littermates will be used in our subsequent studies (Figure 2B). Genotyping was carried out by PCR (online supplemental Figure 1). The protein expression level was further confirmed by western blot and ISCA1 knockout efficiency reached 84.26% in myocardial tissues (Figure 2C and 2D, n = 9 rats per group, P<0.001 *versus* WT).

We then performed the general and the survival rate observation. Cumulative rat mortality data from WT and KO groups were recorded. The survival rate was 100% in the WT group (n=50), while no KO rat (n=16) survived till the end of observation (10 days after birth) (Figure 3A). However, there were no differences in appearance

between WT rats and the KO rats in pups (Figure 3B).

In view of the deaths were clustered between days 7 and days 9 after birth, we thus observed the cardiac structure and function of KO rat at 6.5 days after birth using echocardiography and nuclear magnetic resonance (NMR) (Figure 3C-3D). The KO rat exhibited typical HF phenotypes with larger chambers, thin walls, rapid decreased function of contraction. Those changes were demonstrated by increased left ventricular (LV) diameter both at end diastole and at end systole (LVIDD, LVIDS) (Figure 3E-3F, $P<0.001$ *versus* WT rats), decreased in LV anterior wall thickness both at end diastole and at end systole (LVAWD, LVAWS) (Figure 3G-3H, $P<0.05$, $P<0.01$ *versus* WT rats), decreased LV ejection fraction (LVEF) and LV percent fractional shortening (LVFS) (Figure 3I-3J, $P<0.001$ *versus* WT rats). Online supplemental table 2 showed the data for echocardiographic parameters of LVIDD, LVIDS, LVAWD, LVAWS, LVEF, LVFS and heart rate (HR) from KO and WT groups at 6.5 days of age.

Then hearts from both groups were sampled for gross morphology and hypertrophic markers examination. We found that the overall size increased significantly with ventricular wall collapsed, and the heart weight to body weight ratio (HW/BW) increased obviously in KO group (Figure 3K-3L, $P<0.001$ *versus* WT group). Furthermore, we examined the hypertrophic molecular markers, nppa and nppb, using real-time PCR and found that the expression of these markers increased markedly in heart tissues from the KO group (Figure 3M-3N, $P<0.001$ *versus* WT group).

Taken together, echocardiographic, NMR, histopathology and hypertrophic molecular markers expression examination consistently demonstrated that ISCA1 knockout in myocardium causes severe HF and eventually leads to death in rats.

We then traced the specific time point from which the morphological differences between KO and WT rats occurred. Echocardiography and histopathologic analysis were both performed (Figure 4A-4B. We found that the LV chamber slightly increased, the LV wall decreased, LV function of contraction decreased, which was demonstrated by LVIDS, LVAWS and LVEF, but given no significance, between these two groups at 2.5 days and 0.5 days of age (Figure 4C-4E). We further analyzed two time points in the embryonic period, including E17.5 and E19.5, and it exhibited no difference either with parameters of LV mass and endocardial volume (Figure 4F-4G).

3. ISCA1 deficiency induces oncosis in myocardium

So far, we have found that ISCA1 deficiency induced severe HF through medical imageology and histological observation, and pathological phenotypes were observed including geometric morphology and functional changes,

as larger chambers, thin walls and rapid decreased function of contraction. Therefore, we further examined the histopathological changes of cardiomyocytes from KO rats.

Firstly, histological changes of myocardium were observed by H&E stain at the microscopic level, and we found that myocytes disarray, cellular swelling, cytoplasm swelling and even vacuolation in KO rats compared with the WT rats at 6.5 days of age (Figure 5A, n = 4 rats per group). We subsequently detected morphological changes in the ultrastructure of myocytes in ventricles by transmission electron microscopy (TEM). Poorly organized myocardium, large area of myocardiolysis and disrupted plasma membranes, swollen mitochondria with damaged membrane structure and degeneration of nuclei were observed in KO rats compared with the WT rats at 6.5 days of age (Figure 5B, n = 4 rats per group).

The cardiomyocytes may undergo oncosis in KO rats according to observation at microscopic and ultrastructure level above. Therefore, we further treated the KO rats with the membrane-impermeable Evans blue (EB) dye at 2.5 days and 6.5 days of age, respectively, at which time point were the early and late stages of HF. We found that the dystrophin distributed throughout the sarcolemmal and skeleton in myocardium of WT sections, and no accumulation of EB was observed (Figure 5C). However, smeared dystrophin and EB accumulated were both observed in myocardium sections from KO rats at 2.5 days of age since the destruction of membrane (Figure 5C, n = 3 rats in WT group, n = 3 rats in KO group). Since the increased number of oncosis myocytes, multiple of large area of EB staining were observed in KO rats at 6.5 days of age (Figure 5C, n = 4 rats in WT group, n = 3 rats in KO group), at which time point was the late stages of HF and the membrane structures were also damaged severely.

We then further investigated the morphologic changes of membrane and cytoskeleton in myocardium in KO rat at 6.5 days of age, through colocalization of dystrophin protein and WGA. WGA binds to the membrane lipid and glycoprotein components by cross-linking terminally linked N-acetyl-D-glucosamine in the sarcolemma. The structure of membrane and cytoskeleton in WT rat exhibited clear and intact, however which showed smear and large areas loss in sections from KO rats (Figure 5D, n = 4 rats in WT group, n = 3 rats in KO group).

Taken together, histological observation using H&E stain and TEM, membrane permeability observation through EB treatment and localization observation of membrane and cytoskeleton proteins consistently demonstrated that ISCA1 deficiency induces oncosis in myocardium.

4. ISCA1 deficiency disrupts iron homeostasis in myocardium

In order to find out interacting molecule of ISCA1 and explore the possible molecular mechanisms of pathological phenotypes caused by ISCA1 deletion, immunoprecipitation analysis was subsequently performed.

We first established a stable H9c2 cell line of ISCA1 (using ISCA1-vector within Flag tag, referred as ISCA1-ov) overexpression, then the lysis of cells was used for subsequent co-immunoprecipitation (Co-IP) analysis with Flag antibody (Figure 6A). Finally, we found a molecule interacting with ISCA1, STEAP3, through subsequent western blot (Figure 6B). We then further examined the subcellular localization of ISCA1 and STEAP3 by immunofluorescent staining in myocardium sections from KO rat at 6.5 days of age, and it is demonstrated that ISCA1 and STEAP3 were both expressed in mitochondria of myocardium (Figure 6C).

Previous studies have showed that STEAP3 functions as an iron transporter, and can reduce Fe^{3+} cation as a reductase[29]. Meanwhile, several mechanisms for transporting iron into the mitochondria have been suggested[7, 12, 16, 25, 34, 37]. One of them is the "Kiss and Run" mechanism, that is Fe^{3+} taken up by endocytosis is likely reduced to Fe^{2+} by STEAP3 and directly transported from the endosome to the mitochondria without entering the cytosol. Therefore, we hypothesized that ISCA1 deficiency may affect the interaction between them, and thus affect the level of Fe^{2+} and iron homeostasis in myocardium.

Therefore, we determined the content of Fe^{3+}, Fe^{2+} and total iron in our KO rat. We found that the level of Fe^{2+} decreased, and the level of Fe^{3+} increased in myocardium from KO rats (Figure 6D, $P<0.05$, $P<0.01$ *versus* WT rats). While the level of total iron given no change compared with the WT group (Figure 6D). This result indicated that iron steady state was seriously affected with the deletion of ISCA1 in myocardium from rats.

We then established a stable H9c2 cell line with STEAP3 knockdown expression (with STEAP3-shRNA vector, referred as STEAP3-kd) to verify in reverse the iron regulation affected by the interaction between ISCA1 and STEAP3. The knockdown ratio of STEAP3 protein is 67.24% and both of the expression of ISCA1 and STEAP3 decreased significantly in the stable STEAP3-kd cell line (Figure 6E-6F, $P<0.001$ *versus* empty-vector control).

Since the homeostasis of iron ion in myocardium was seriously affected by ISCA1 deletion, then we investigated whether the Fe^{2+} obtained directly by ISCA1 would change. Meanwhile, the concentration of Fe^{2+} will decrease after the expression of STEAP3 is down-regulated, we specially add Fe^{3+} (ferric ammonium citrate (FAC)) to observe the dynamic change of Fe^{2+} obtained directly by ISCA1 at this time. The empty-vector stably cells and STEAP3-Kd stably cells groups were first collected for co-immunoprecipitation with ISCA1 antibody, the co-IP product was then detected for iron concentration after FAC stimulation (100 μM). We found that ISCA1 protein yields significantly less Fe^{2+} with STEAP3 knockdown (Figure 6G, $P<0.05$, *versus* empty-vector control).

So far, we found that ISCA1 interacted with STEAP3 and their expression are directly related. ISCA1 deficiency affect seriously the steady state of iron ions. The Fe^{2+} obtained by ISCA1 decreased significantly with

STEAP3 expression knockdown. These results suggested that ISCA1 plays an important role in the regulation of iron homeostasis in myocardium, and STEAP3 is involved in the process of obtaining Fe^{2+} by ISCA1.

5. ISCA1 plays an important role in energy metabolism of myocardial mitochondrial respiratory chain

We subsequently detected the expression level of markers and enzyme activity for complex I, II and IV in our model rat. We found that mitochondrial complex I subunit, NADH: ubiquinone oxidoreductase subunit A9 (NDUFA9) and NADH: ubiquinone oxidoreductase core subunit S3 (NDUFS3), and complex II subunit, succinate dehydrogenase complex iron sulfur subunit B (SDHB), were obviously decreased in myocardium from KO rats through western blot (Figure 7A-7D, $P<0.001$, *versus* WT group). And the enzyme activity of complex I, II and IV also decreased significantly in myocardium from KO rats (Figure 7E-7G, $P<0.01$, $P<0.001$, *versus* WT group). And we found that ubiquinol-cytochrome c reductase core protein 2 (UQCRC2, respiratory chain complex III marker enzymes), cytochrome c oxidase subunit 4 (COX IV, a critical component of the mitochondrial respiratory pathway), aconitase 2 (ACO2, one of the mitochondrial matrix proteins) given no change in myocardium from KO rats compared with WT rats (online supplemental Figure 2A-2D).

Meanwhile, ATP generation was detected, and the concentration decreased obviously in myocardium from KO rats (Figure 7H, $P<0.001$, *versus* WT group). Therefore, the function of mitochondrial complex and energy generation in myocardium were severely impaired due to ISCA1 deficiency.

Subsequently, we performed the calcein-AM/propidium iodide cell-survival assay, the dead cell number increased in STEAP3-kd group compared with the empty-vector group (Figure 7I-7J, $P<0.001$, *versus* empty-vector group), and which were significantly reversed by increased expression of ISCA1 (Figure 7I-7J, $P<0.001$, STEAP3-kd+ISCA1-Flag plasmid group *versus* STEAP3-kd group). With the knockdown of STEAP3 *in vitro*, the ATP generation were also decreased obviously (Figure 7K, $P<0.01$, *versus* empty-vector group). When stimulated by ISCA1-flag-plasmid, the ATP generation were partially compensated (Figure 7 K, $P<0.05$, STEAP3-kd+ISCA1-Flag-plasmid group *versus* STEAP3-kd group).

Furthermore, the oncosis phenotypes of membrane and structural damage (online supplemental Figure 2E) and the increased expression of hypertrophic markers induced by STEAP3 knockdown were also partially compensated by ISCA1-flag-plasmid stimulation (Figure 7L, $P<0.05$, STEAP3-kd+ISCA1-Flag-plasmid group *versus* STEAP3-kd group).

Discussion

In this study, conditional *Isca1* knockout (cKO) rats was established with CRISPR/Cas9 technology, and then ISCA1 was selectively eliminated in myocardium by cross mating of cKO rats to *α-MHC-Cre* tool rats. We then investigated the effects of ISCA1 deficiency on cardiac development, myocardial energy metabolism, and its possible molecular mechanisms.

We found that ISCA1 deletion cause severe HF through echocardiography analysis, NMR analysis and histological analysis, and KO rats will be died within 10 days of age. Meanwhile, the cardiomyocytes from KO rats represented as oncosis by using histology, EB staining and cell skeleton colocalization analysis. At the same time, we investigated the possible molecular mechanism of pathological phenotypes *in vivo*. We determined that ISCA1 interacts with STEAP3, a member of the oxidoreductase family, through immunoprecipitation analysis and subsequent molecular validation in reverse. We then found that the level of Fe^{2+} obtained by ISCA1 decreased obviously with STEAP3 knockdown regulated, and further the level of Fe^{3+} and Fe^{2+} undergo different degrees of regulation, and the iron homeostasis suffered a destruction in myocardium with ISCA1 deficiency. Whereafter, the subunit or enzyme activities of myocardial mitochondrial complex I, II and IV were significantly affected, indicating impaired mitochondrial function, and the structure and morphology of mitochondria were also severely impaired by transmission electron microscopy. Meanwhile, ATP production decreased significantly, indicating that the myocardial energy supply was seriously insufficient. In the reverse validation experiment in vitro, cell death and hypertrophic markers induced by STEAP3 knockdown regulated could be partially ameliorated by administration of ISCA1. In summary, ISCA1 deficiency in myocardium caused impair on iron metabolism, and then mitochondrial respiratory chain and energy metabolism damaged, and cardiomyocytes oncosis occurred due to energy shortage, and eventually lead to HF and body death.

The heart is highly dependent on mitochondrial metabolism to meet its tremendous energy requirements. In fact, >40% of the cytoplasmic space[14] in adult cardiac myocytes is occupied by mitochondria, which densely packed between sarcomeres and around the nucleus[8]. Maintaining a healthy mitochondrial population is of paramount importance for cardiac homeostasis, since damaged mitochondria produce less ATP and generate dangerous amounts of reactive oxygen species (ROS). Accumulated ROS may damage mitochondrial DNA, membrane lipids and respiratory complex proteins, leading to a catastrophic feedforward cycle of oxidative damage and ultimately cell death[45]. This general mechanism is particularly relevant to terminally-differentiated tissues such as the brain and heart, as demonstrated in neurodegenerative and cardiovascular diseases[18, 24].

Mutations in the genes involved in synthesis of ISC may severely impair diverse mitochondrial metabolic

pathways and interfere with energy production[2, 6, 27]. Meanwhile, gene mutation involved in ISC synthesis is closely related to MMDS. According to genes involved in this disease, ISCA1 abnormal caused type of MMDS5. Previous studies have shown that oncosis occurs due to lack of energy[17, 30]. Therefore, our present work and previous research reports proved that ISCA1 is essential for heart development, and the mechanism is all relevant to energy metabolism disorder induced by mitochondrial dysfunction.

It is reported that abnormal muscle or heart development was observed in MMDS2 , MMDS3 , MMDS5 and MMDS6 subtypes. Patients carrying BOLA3 mutations presented with optic atrophy, cardiomyopathy, diabetes and diarrhea[1, 28, 42] ISCA1 is crucial for the maturation of [4Fe-4S] protein in skeletal muscle. In addition, previous reports also showed that ISC protein-associated phenotypes mainly include diverse metabolic abnormal, at the cellular level, it exhibited as abnormal respiratory chain and iron metabolism in mitochondria[9].

Therefore, our findings are consistent with the phenotypes found in clinical patients with MMDS. Our results demonstrated the important role of ISCA1 gene in heart development *in vivo*. as ISCA1 deletion induces severe HF and the cardiomyocytes represented as oncosis. Meanwhile, the level of Fe^{3+} and Fe^{2+} undergo different degrees of regulation, and the iron homeostasis suffered a destruction in myocardium with ISCA1 deficiency.

As a result, first of all, the subsequent metabolic processes that Fe^{2+} involved, including the synthesis of mitochondria [4Fe-4S] and Fe/S cluster transported to the cytoplasm, are affected, then, it affects energy generation (Figure 8).

In this paper, we determined STEAP3, a new interaction molecular of ISCA1, through immunoprecipitation and immunoblotting analysis. Members from STEAP3 family exhibited different expressional profiles. STEAP1 and STEAP2 are highly expressed in the prostate gland, and was found to be closely associated with prostate cancer metastasis[31, 47]. STEAP4 is highly expressed in adipose tissue and is a co-regulator of nutrients and inflammation[44]. STEAP3 is expressed in the liver, duodenum, skeletal muscle and heart, and has been found to be a potential tumor suppressor gene, as well as be involved in exosome secretion[10]. STEAP3 deficiency resulted in anemia and severe iron metabolism disorder in mice[10].

By retrieving display with GeneCards (http://www.genecards.org), STEAP3 were mainly located in endosome, plasma membrane and mitochondrion and so on. In this paper, we found that ISCA1 and STEAP3 are coexpressed in mitochondria, in addition, one of the multiple mechanisms for transporting iron into mitochondria is the "Kiss and Run" mechanism: Fe^{3+} taken up by endocytosis is likely reduced to Fe^{2+} by STEAP3 and directly transported from the endosome to the mitochondria without entering the cytosol[7, 12, 16, 25, 34, 37]. Meanwhile,

we found that level of Fe^{2+} obtained by ISCA1 decreased obviously with STEAP3 knockdown regulated. Therefore, we speculated that these two molecules interact with each other on the mitochondrial membrane, and STEAP3 plays important role in the process of obtaining Fe^{2+} by ISCA1 (Figure 8).

In addition, in a recent report, substantial decrease of mitochondrial [4Fe-4S] containing proteins, including aconitase 2 (ACO2), complex II (SDHB) and two subunits of complex I (NDUFS3 and NDUFS5) was observed after ISCA1 knockdowns in the skeletal muscles of mice[4]. However, in our study, we found that NDUFA9, NDUFS3 and SDHB decreased significantly in heart tissues from KO rats, while ACO2 and subunits of complex III (UQCRC2) exhibited no change. Our present work and the study mentioned above suggested that expressional characteristic of [4Fe-4S] containing proteins effected by ISCA1 exists differences in different tissues.

In our study, ISCA1 deficiency in myocardium caused impair on iron metabolism, and then mitochondrial respiratory chain and energy metabolism damaged, and cardiomyocytes oncosis occurred due to energy shortage, and eventually lead to HF and body death. Meanwhile, STEAP3, the interacting molecules with ISCA1, plays important role in the process of obtaining Fe^{2+} by ISCA1. Taken together, this study was the first to verify the effect of ISCA1 gene deletion on cardiac development *in vivo*, providing laboratory evidence for the effect and the possible mechanisms of MMDS induced by abnormal expression of genes related to iron sulfur cluster biosynthesis on cardiac development. Therefore, the results in this paper provide basis for further investigation of the pathogenesis of MMDS and new clues for searching of clinical therapeutic targets.

Online supplemental materials

Table. S1 shows the sequences of the primers in this study.

Table. S2 shows the echocardiographic parameters of ISCA1-KO rat at 6.5 days of age.

Figure. S1 shows the genotyping assay for ISCA1-KO rat through PCR.

Figure S2 shows the expression of several mitochondrial respiratory chain proteins and the oncosis phenotype in reverse validation *in vitro*.

Acknowledgments The authors thank the following persons and institutions: Yajun Yang, Beijing Key Laboratory of Active Substance Discovery and Drug ability Evaluation Institute of Material Medical Chinese Academy of Medical Sciences and Peking Union Medical College, Beijing, China, for discussion regarding iron ion measurement. Qing Xu, Core Facilities for Electrophysiology, Core Facilities Center, Capital Medical University, Beijing, China, for advices on echocardiographic analysis for our genetically modified rats. He Wang, College of Life sciences and Bioengineering, Beijing Jiaotong University, Beijing, China, for preparation and phenotypes discussion for transmission electron microscope samples.

Funding This work was supported by CAMS Innovation Fund for Medical Sciences (CIFMS, 2016-I2M-1-015), the Beijing Natural Science Foundation (5212017), National Natural Science Foundation (31872314 and 31970508)

Author contributions

Dan Lu and Lianfeng Zhang conceived the study. Yahao Ling and Xinlan Yang did most of the experiments.Yuanwu Ma and Xu Zhang contributed to establishment of the animal models and sequence analysis. Wei Chen contributed to microinjection technique. Wei Dong and Kai Gao contributed to echocardiography and NMR analysis. Xiaolong Qi and Jing Li contributed to immunofluorescence assay. Feifei Guan contributed to cell expeiment. Mengdi Liu, Jiaxin Ma and Xiaoyu Jiang contributed to gennotype identification and plasmid preparation. Shan Gao and Xiang Gao and Shuo Pan contributed to the animal breeding and management. Dan Lu wrote the mauscript with feedback from all authors, and Jizheng Wang contributed to writing editing.

Data availability The data that support the findings of this study are available from the corresponding author upon reasonable request.

Compliance with ethical standards

Ethical approval All experiments were reviewed and approved by the Animal Care and Use Committee of the Institute of Laboratory Animal Science of Peking Union Medical College.

Conflict of interest

The authors have no conflict of interest to declare.

References

1. Ahting U, Mayr JA, Vanlander AV, Hardy SA, Santra S, Makowski C, Alston CL, Zimmermann FA, Abela L, Plecko B (2015) Clinical, biochemical, and genetic spectrum of seven patients with NFU1 deficiency. Front. Genet 6:123. https://doi.org/10.3389/fgene.2015.00123
2. Ajit Bolar N, Vanlander AV, Wilbrecht C, Van der Aa N, Smet J, De Paepe B, Vandeweyer G, Kooy F, Eyskens F, De Latter E (2013) Mutation of the iron-sulfur cluster assembly gene IBA57 causes severe myopathy and encephalopathy. Hum. Mol. Genet. 22:2590-2602. https://doi.org/10.1093/hmg/ddt107
3. Al-Hassnan ZN, Al-Dosary M, Alfadhel M, Faqeih EA, Alsagob M, Kenana R, Almass R, Al-Harazi OS, Al-Hindi H, Malibari OI (2015) ISCA2 mutation causes infantile neurodegenerative mitochondrial disorder. J. Med. Genet. 52:186-194. https://doi.org/10.1136/jmedgenet-2014-102592
4. Beilschmidt LK, de Choudens SO, Fournier M, Sanakis I, Hograindleur M-A, Clémancey M, Blondin G, Schmucker S, Eisenmann A, Weiss A (2017) ISCA1 is essential for mitochondrial Fe 4 S 4 biogenesis in vivo. Nat. Commun. 8:15124. https://doi.org/10.1038/ncomms15124
5. Beilschmidt LK, Puccio HM (2014) Mammalian Fe-S cluster biogenesis and its implication in disease. Biochimie 100:48-60. https://doi.org/10.1016/j.biochi.2014.01.009
6. Cameron JM, Janer A, Levandovskiy V, MacKay N, Rouault TA, Tong W-H, Ogilvie I, Shoubridge EA, Robinson BH (2011) Mutations in iron-sulfur cluster scaffold genes NFU1 and BOLA3 cause a fatal deficiency of multiple respiratory chain and 2-oxoacid dehydrogenase enzymes. Am. J. Hum. Genet. 89:486-495. https://doi.org/10.1016/j.ajhg.2011.08.011
7. Devireddy LR, Hart DO, Goetz DH, Green MR (2010) A mammalian siderophore synthesized by an enzyme with a bacterial homolog involved in enterobactin production. Cell 141:1006-1017. https://doi.org/10.1016/j.cell.2010.04.040
8. Dorn GW, Vega RB, Kelly DP (2015) Mitochondrial biogenesis and dynamics in the developing and diseased heart. Genes Dev. 29:1981-1991. https://doi.org/10.1101/gad.269894.115
9. Frazier AE, Thorburn DR, Compton AG (2019) Mitochondrial energy generation disorders: genes, mechanisms, and clues to pathology. J. Biol. Chem. 294:5386-5395. https://doi.org/10.1074/jbc.R117.809194
10. Grandchamp B, Hetet G, Kannengiesser C, Oudin C, Beaumont C, Rodrigues-Ferreira S, Amson R, Telerman A, Nielsen P, Kohne E (2011) A novel type of congenital hypochromic anemia associated with a nonsense mutation in the STEAP3/TSAP6 gene. Blood 118:6660-6666. https://doi.org/10.1182/blood-2011-01-329011
11. Guan F, Yang X, Li J, Dong W, Zhang X, Liu N, Gao S, Wang J, Zhang L, Lu D (2019) New molecular mechanism underlying myc-mediated cytochrome p450 2e1 upregulation in apoptosis and energy metabolism in the myocardium. J. Am. Heart. Assoc. 8:e009871. https://doi.org/10.1161/JAHA.118.009871
12. Hamdi A, Roshan TM, Kahawita TM, Mason AB, Sheftel AD, Ponka P (2016) Erythroid cell mitochondria receive endosomal iron by a "kiss-and-run" mechanism. Biochim. Biophys.

Acta 1863:2859-2867. https://doi.org/10.1016/j.bbamcr.2016.09.008

13. Hasumi Y, Baba M, Hasumi H, Huang Y, Lang M, Reindorf R, Oh H-b, Sciarretta S, Nagashima K, Haines DC (2014) Folliculin (Flcn) inactivation leads to murine cardiac hypertrophy through mTORC1 deregulation. Hum. Mol. Genet. 23:5706-5719. https://doi.org/10.1093/hmg/ddu286
14. Hom J, Sheu S-S (2009) Morphological dynamics of mitochondria—a special emphasis on cardiac muscle cells. J. Mol. Cell. Cardiol. 46:811-820. https://doi.org/10.1016/j.yjmcc.2009.02.023
15. Kido M, Otani H, Kyoi S, Sumida T, Fujiwara H, Okada T, Imamura H (2004) Ischemic preconditioning-mediated restoration of membrane dystrophin during reperfusion correlates with protection against contraction-induced myocardial injury. Am. J. Physiol. Heart. Circ. Physiol. 287:81-90. https://doi.org/10.1152/ajpheart.01140.2003
16. Lange H, Kispal G, Lill R (1999) Mechanism of iron transport to the site of heme synthesis inside yeast mitochondria. J. Biol. Chem. 274:18989-18996. https://doi.org/10.1074/jbc.274.27.18989
17. Liu H, He Z, Germič N, Ademi H, Frangež Ž, Felser A, Peng S, Riether C, Djonov V, Nuoffer J-M (2020) ATG12 deficiency leads to tumor cell oncosis owing to diminished mitochondrial biogenesis and reduced cellular bioenergetics. Cell Death Differ. 27:1965-1980. https://doi.org/10.1038/s41418-019-0476-5
18. López-Otín C, Blasco MA, Partridge L, Serrano M, Kroemer G (2013) The hallmarks of aging. Cell 153:1194-1217. https://doi.org/10.1016/j.cell.2013.05.039
19. Lu D, Ma Y, Zhang W, Bao D, Dong W, Lian H, Huang L, Zhang L (2012) Knockdown of cytochrome P450 2E1 inhibits oxidative stress and apoptosis in the cTnTR141W dilated cardiomyopathy transgenic mice. Hypertension 60:81-89. https://doi.org/10.1161/HYPERTENSIONAHA.112.191478
20. Lu D, Wang J, Li J, Guan F, Zhang X, Dong W, Liu N, Gao S, Zhang L (2018) Meox1 accelerates myocardial hypertrophic decompensation through Gata4. Cardiovasc. Res. 114:300-311. https://doi.org/10.1093/cvr/cvx222
21. Lu D, Zhang L, Bao D, Lu Y, Zhang X, Liu N, Ge W, Gao X, Li H, Zhang L (2014) Calponin1 inhibits dilated cardiomyopathy development in mice through the εPKC pathway. Int. J. Cardiol. 173:146-153. https://doi.org/10.1016/j.ijcard.2014.02.032
22. Ma Y, Yu L, Pan S, Gao S, Chen W, Zhang X, Dong W, Li J, Zhou R, Huang L (2017) CRISPR/Cas9‐mediated targeting of the Rosa26 locus produces Cre reporter rat strains for monitoring Cre‐loxP‐mediated lineage tracing. FEBS. J. 284:3262-3277. https://doi.org/10.1111/febs.14188
23. Ma Y, Zhang X, Shen B, Lu Y, Chen W, Ma J, Bai L, Huang X, Zhang L (2014) Generating rats with conditional alleles using CRISPR/Cas9. Cell Res. 24:122-125. https://doi.org/10.1038/cr.2013.157
24. Morales PE, Arias-Durán C, Ávalos-Guajardo Y, Aedo G, Verdejo HE, Parra V, Lavandero S (2020) Emerging role of mitophagy in cardiovascular physiology and pathology. Mol. Aspects Med. 71:100822. https://doi.org/10.1016/j.mam.2019.09.006
25. Mühlenhoff U, Molik S, Godoy JR, Uzarska MA, Richter N, Seubert A, Zhang Y, Stubbe J, Pierrel F, Herrero E (2010) Cytosolic monothiol glutaredoxins function in intracellular iron sensing and trafficking via their bound iron-sulfur cluster. Cell

Metab. 12:373-385. https://doi.org/10.1016/j.cmet.2010.08.001

26. Nagahama K, Kimura Y, Takemoto A (2018) Living functional hydrogels generated by bioorthogonal cross-linking reactions of azide-modified cells with alkyne-modified polymers. Nat. Commun. 9:1-11. https://doi.org/10.1038/s41467-018-04699-3

27. Navarro-Sastre A, Tort F, Stehling O, Uzarska MA, Arranz JA, del Toro M, Labayru MT, Landa J, Font A, Garcia-Villoria J (2011) A fatal mitochondrial disease is associated with defective NFU1 function in the maturation of a subset of mitochondrial Fe-S proteins. Am. J. Hum. Genet. 89:656-667. https://doi.org/10.1016/j.ajhg.2011.10.005

28. Nishioka M, Inaba Y, Motobayashi M, Hara Y, Numata R, Amano Y, Shingu K, Yamamoto Y, Murayama K, Ohtake A (2018) An infant case of diffuse cerebrospinal lesions and cardiomyopathy caused by a BOLA3 mutation. Brain Dev. 40:484-488. https://doi.org/10.1016/j.braindev.2018.02.004

29. Ohgami RS, Campagna DR, McDonald A, Fleming MD (2006) The Steap proteins are metalloreductases. Blood 108:1388-1394. https://doi.org/10.1182/blood-2006-02-003681

30. Peters AA, Jamaludin SY, Yapa KT, Chalmers S, Wiegmans AP, Lim HF, Milevskiy MJ, Azimi I, Davis FM, Northwood KS (2017) Oncosis and apoptosis induction by activation of an overexpressed ion channel in breast cancer cells. Oncogene 36:6490-6500. https://doi.org/10.1038/onc.2017.234

31. Porkka KP, Helenius MA, Visakorpi T (2002) Cloning and characterization of a novel six-transmembrane protein STEAP2, expressed in normal and malignant prostate. Lab. Invest. 82:1573-1582. https://doi.org/10.1097/01.lab.0000038554.26102.c6

32. Redondo-Angulo I, Mas-Stachurska A, Sitges M, Giralt M, Villarroya F, Planavila A (2016) C/EBPβ is required in pregnancy-induced cardiac hypertrophy. Int. J. Cardiol. 202:819-828. https://doi.org/10.1016/j.ijcard.2015.10.005

33. Sheftel AD, Wilbrecht C, Stehling O, Niggemeyer B, Elsässer H-P, Mühlenhoff U, Lill R (2012) The human mitochondrial ISCA1, ISCA2, and IBA57 proteins are required for [4Fe-4S] protein maturation. Mol. Biol. Cell 23:1157-1166. https://doi.org/10.1091/mbc.E11-09-0772

34. Sheftel AD, Zhang A-S, Brown C, Shirihai OS, Ponka P (2007) Direct interorganellar transfer of iron from endosome to mitochondrion. Blood 110:125-132. https://doi.org/10.1182/blood-2007-01-068148

35. Shukla A, Hebbar M, Srivastava A, Kadavigere R, Upadhyai P, Kanthi A, Brandau O, Bielas S, Girisha KM (2017) Homozygous p.(Glu87Lys) variant in ISCA1 is associated with a multiple mitochondrial dysfunctions syndrome. J. Hum. Genet. 62:723-727. https://doi.org/10.1038/jhg.2017.35

36. Shukla A, Kaur P, Girisha KM (2018) Report of the third family with multiple mitochondrial dysfunctions syndrome 5 caused by the founder variant p.(Glu87Lys) in ISCA1. J. Pediatr. Genet. 7:130-133. https://doi.org/10.1055/s-0038-1641177

37. Shvartsman M, Kikkeri R, Shanzer A, Cabantchik ZI (2007) Non-transferrin-bound iron reaches mitochondria by a chelator-inaccessible mechanism: biological and clinical implications. American Journal of Physiology-Cell Physiology 293:C1383-C1394. https://doi.org/10.1152/ajpcell.00054.2007

38. Stehling O, Wilbrecht C, Lill R (2014) Mitochondrial iron–sulfur protein biogenesis and human disease. Biochimie 100:61-77. https://doi.org/10.1016/j.biochi.2014.01.010

39. Tadokoro T, Ikeda M, Ide T, Deguchi H, Ikeda S, Okabe K, Ishikita A, Matsushima S, Koumura T, Yamada K-i (2020) Mitochondria-dependent ferroptosis plays a pivotal role in doxorubicin cardiotoxicity. JCI insight 5. https://doi.org/10.1172/jci.insight.132747
40. Tong M, Sadoshima J (2016) Mitochondrial autophagy in cardiomyopathy. Curr. Opin. Genet. Dev. 38:8-15. https://doi.org/10.1016/j.gde.2016.02.006
41. Torraco A, Stehling O, Stümpfig C, Rösser R, De Rasmo D, Fiermonte G, Verrigni D, Rizza T, Vozza A, Di Nottia M (2018) ISCA1 mutation in a patient with infantile-onset leukodystrophy causes defects in mitochondrial [4Fe-4S] proteins. Hum. Mol. Genet. 27:2739-2754. https://doi.org/10.1093/hmg/ddy273
42. Uzarska MA, Nasta V, Weiler BD, Spantgar F, Ciofi-Baffoni S, Saviello MR, Gonnelli L, Mühlenhoff U, Banci L, Lill R (2016) Mitochondrial Bol1 and Bol3 function as assembly factors for specific iron-sulfur proteins. Elife 5:e16673. https://doi.org/10.7554/eLife.16673
43. Vögtle F-N, Brändl B, Larson A, Pendziwiat M, Friederich MW, White SM, Basinger A, Kücükköse C, Muhle H, Jähn JA (2018) Mutations in PMPCB encoding the catalytic subunit of the mitochondrial presequence protease cause neurodegeneration in early childhood. Am. J. Hum. Genet. 102:557-573. https://doi.org/10.1016/j.ajhg.2018.02.014
44. Wellen KE, Fucho R, Gregor MF, Furuhashi M, Morgan C, Lindstad T, Vaillancourt E, Gorgun CZ, Saatcioglu F, Hotamisligil GS (2007) Coordinated regulation of nutrient and inflammatory responses by STAMP2 is essential for metabolic homeostasis. Cell 129:537-548. https://doi.org/10.1016/j.cell.2007.02.049
45. Whelan RS, Kaplinskiy V, Kitsis RN (2010) Cell death in the pathogenesis of heart disease: mechanisms and significance. Annu. Rev. Physiol. 72:19-44. https://doi.org/10.1146/annurev.physiol.010908.163111
46. Wu T-T, Ma Y-W, Zhang X, Dong W, Gao S, Wang J-Z, Zhang L-F, Lu D (2020) Myocardial tissue-specific Dnmt1 knockout in rats protects against pathological injury induced by Adriamycin. Lab. Invest. 100:974-985. https://doi.org/10.1038/s41374-020-0402-y
47. Yang D, Holt GE, Velders MP, Kwon ED, Kast WM (2001) Murine six-transmembrane epithelial antigen of the prostate, prostate stem cell antigen, and prostate-specific membrane antigen: prostate-specific cell-surface antigens highly expressed in prostate cancer of transgenic adenocarcinoma mouse prostate mice. Cancer Res. 61:5857-5860. https://doi.org/10.1097/00002820-200108000-00015
48. Yang X, Lu D, Zhang X, Chen W, Gao S, Dong W, Ma Y, Zhang L (2019) Knockout of ISCA 1 causes early embryonic death in rats. Animal. Model. Exp. Med. 2:18-24. https://doi.org/10.1002/ame2.12059
49. Yang Y, Luo M, Zhang K, Zhang J, Gao T, O'Connell D, Yao F, Mu C, Cai B, Shang Y (2020) Nedd4 ubiquitylates VDAC2/3 to suppress erastin-induced ferroptosis in melanoma. Nat. Commun. 11:433. https://doi.org/10.1038/s41467-020-14324-x
50. Yao X, Wigginton JG, Maass DL, Ma L, Carlson D, Wolf SE, Minei JP, Zang QS (2014) Estrogen-provided cardiac protection following burn trauma is mediated through a reduction in mitochondria-derived DAMPs. Am. J. Physiol. Heart. Circ. Physiol. 306:882-894. https://doi.org/10.1152/ajpheart.00475.2013

Figure legends

Figure 1. ISCA1 is induced under cardiomyopathy and heart failure and expressed in myocardial mitochondria. ISCA1 expression in heart tissues from adriamycin (ADR) treated and thoracic aorta constriction (TAC) mice models using GAPDH as normalization (**A-B**, *n*=4 mice per group, ***P<0.001 *versus* respective control). ISCA1 expression in heart tissues from hypertrophic cardiomyopathy (HCM) patients and healthy heart donors using GAPDH as normalization **(C-D**, *n*=4 in normal and *n*=5 in HCM patients, ***P<0.001 *versus* normal). Immunofluorescence detection of ISCA1 and mitochondrial marker of VDAC1 in the heart tissues of WT rats at 2 weeks of age (**E**, n=4 rats per group, white scale bar = 5 μm).

Figure 2. Establishment and identification for myocardial tissue specific knockout of Isca1 rat. *Isca1* conditional knockout (*Isca1* cKO) rats were generated by utilizing the *Cre-loxP* recombination system **(A)**, which were then put two generation of cross mating with the *α-MHC-Cre* rats, and rats with myocardial tissue specific knockout of ISCA1 were obtained, referred as *Isca1*-KO (*Isca1*$^{flox/flox}$/*α-MHC-Cre*) **(B)**. The ISCA1 expression **(C)** in heart tissues from KO rat was detected using western blot **(C-D**, n = 9 rats per group, ***P<0.001 *versus* WT; LA: left arm, RA: right arm).

Figure 3. Myocardial specific ISCA1 deficiency induces severe HF in rats. Cumulative percent survival rate for WT (n=50) and KO (n=16) groups were calculated from 0 to 10 days after birth **(A)**. Photographs of rats from WT and KO groups at 6.5 days of age **(B)**. The M-mode echocardiography screenshot **(C)** and nuclear magnetic resonance (NMR) screenshot **(D**, white scale bar = 5 mm**)** from WT and KO groups at 6.5 days of age. Echocardiographic parameters of LVIDD, LVIDS, LVAWD, LVAWS, EF, and FS were analyzed in rats from both groups at 6.5 days of age (**E-J**, n=8 in WT group and n=9 in KO group, *P < 0.05, **P< 0.01, ***P<0.001 *versus* WT). Photograph of heart after dissection in rat from both groups at 6.5 days of age **(K)** and the heart weight to body weight (HW/BW) ratio was calculated (**L**, n=31 in WT group and n=29 in KO group, **P<0.01 *versus* WT). Quantitative analysis of nppa and nppb mRNA levels in myocardium from rats in both groups at 6.5 days of age by real-time PCR (**M-N**, n=6 rats per group, ***P<0.001 *versus* WT).

Figure 4. Trace the starting point of morphological differences. The M-mode echocardiography screenshot in both groups at 0.5 and 2.5 days after birth, and in the embryonic period of E17.5 and E19.5 **(A)**. Representative photographs of the whole-heart longitudinal sections with H&E staining from both groups (**B**,

black bar=2 mm). Echocardiographic parameters of LVIDS, LVAWS, FS, LV Mass, and endocardial volume were analyzed in rat from both groups at 6.5 days of age (**C-G**, ns: not significant).

Figure 5. ISCA1 deficiency induces oncosis in myocardium.

Representative photographs of the whole-heart longitudinal sections and its magnification with H&E staining from rats of WT and KO groups at 6.5 days of age (**A**, n = 4 rats per group, black bar=2 mm, white bar= 20 μm). Transmission electron microscope (TEM) analysis of left ventricular free walls from rats of WT and KO groups at 6.5 days of age (**B**, n = 4 rats per group, open orange arrow: mitochondria, open blue arrow: sarcomere, open green arrow: nuclear). Representative photographs of immunofluorescence staining for dystrophin and Evans blue (EB) (**C**, n = 3 rats in WT group and n = 3 rats in KO group at 2.5 days of age, n = 4 rats in WT group and n = 3 rats in KO group at 6.5 days of age, yellow bar=20 μm, open white arrow: EB stain positive area). Representative photographs of immunofluorescence staining for dystrophin and wheat germ agglutinin (WGA) **(D**, n = 4 rats in WT group, n = 3 rats in KO group, yellow bar=20 μm).

Figure 6. ISCA1 deficiency disrupts iron homeostasis in myocardium

Screening processes for finding interacting molecules with ISCA1 using co-immunoprecipitation (Co-IP) and western blot analysis (**A**). Western blot verification for six-transmembrane epithelial antigen of prostate 3 (STEAP3), a molecule interacting with ISCA1 (**B**). Representative photographs of immunofluorescence staining for ISCA1 and STEAP3 in myocardium sections from wt rat at 6.5 days of age (C, n = 3 rats per group, white bar=5 μm). The total iron, ferrous iron (Fe^{2+}) and ferric iron (Fe^{3+}) levels in heart tissues of WT and KO rats were detected by colorimetry (**D**, n = 4 rats per group, $*P < 0.05$, $**P< 0.01$, *versus* WT group). The expression of STEAP3 and ISCA1 in empty-vector stably H9c2 cells and STEAP3-Kd stably H9c2 cells were detected using western blot (**E).** Quantitative analysis of ISCA1 and STEAP3 expression using GAPDH for normalization (**F,** n = 4 rats per group, $***P< 0.001$, *versus* empty-vector group**)**. The Fe^{2+} levels in both stably cells of empty-vector and STEAP3-Kd groups were detected by colorimetry after stimulation by ferric ammonium citrate (100 μM) in immunoprecipitation product pulled down by ISCA1 antibody **(G)** (*$P<0.05$, *versus* empty-vector group).

Figure 7. ISCA1 plays an important role in energy metabolism of myocardial mitochondrial respiratory chain. The expression level of NDUFA9 and NDUFS3 and SDHB were detected in myocardium from KO rats at 6.5 days of age through western blot (**A**). Quantitative analysis of NDUFA9, NDUFS3 and SDHB expression

using TOMM20 for normalization **(B-D**, n=4 in WT group and n=5 in KO group，***P<0.001, *versus* WT group**).** The enzyme activity of complex I, II and IV were detected in myocardium from KO rats using colorimetric method (**E-G**, **P<0.01, ***P<0.001, *versus* WT group). The ATP generation in myocardial tissue from KO rat at 6.5 days of age was determined by colorimetry (**H**, n=4 in WT group and n=5 in KO group, ***P<0.001, *versus* WT group). Representative images of calcein AM/propidium iodide (PI) double staining in H9c2 cells of four group (**I**, empty-vector: stable empty-vector cells; STEAP3-Kd: stable STEAP3-Kd cells; empty-vector+ISCA1-Flag-plasmid: ISCA1-Flag plasmid was transient transfected to stable empty-vector cells; STEAP3-Kd+ISCA1-Flag-plasmid: ISCA1-Flag plasmid was transient transfected to stable STEAP3-Kd cells). Percentage of live cells/dead cells number after calcein AM/propidium iodide (PI) double staining (**J**, repeated assay three times independently, ***P<0.001, STEAP3-Kd group *versus* empty-vector group, $^{\#\#\#}P$<0.001, STEAP3-Kd+ISCA1-Flag-plasmid group *versus* STEAP3-Kd group). The ATP generation in H9c2 cells of four groups were determined by colorimetry (**K**, repeated assay three times independently, **P<0.01, STEAP3-Kd group *versus* empty-vector group, $^{\#}P$<0.05, STEAP3-Kd+ISCA1-Flag-plasmid group *versus* STEAP3-Kd group). Quantitative analysis of nppa at mRNA levels in H9c2 cells from four groups were assayed by real-time PCR (**L**, repeated assay three times independently, ***P<0.001, STEAP3-Kd group *versus* empty-vector group, $^{\#}P$<0.05, STEAP3-Kd+ISCA1-Flag-plasmid group *versus* STEAP3-Kd group).

Figure 8. Schematic illustrating the alteration of iron metabolism in cytoplasm and mitochondrial due to the deficiency of ISCA1 in myocardium of KO rat. ISCA1 performed important role in maturation of mitochondrial [4Fe-4S] proteins in previous reports, thus, providing the basic assembly element for the formation of cytoplasm and mitochondrial Fe/S complex. We found that ISCA1 interacts with STEAP3 (Six-Transmembrane Epithelial Antigen of Prostate 3, functions as an iron transporter and reduce Fe^{3+} cation as a metalloreductase), and Fe^{2+} obtained by ISCA1 reduced significantly with STEAP3 knowdown regulated. Meanwhile, we found that the level of Fe^{3+} and Fe^{2+} undergo different degrees of regulation, and the iron homeostasis suffered a destruction in myocardium with ISCA1 deficiency. The experimental results above suggested us that the interaction between ISCA1 and STEAP3 was seriously affected in the “Kiss and Run” mechanism (one of the five main mechanisms for transporting iron into the mitochondria) and Fe^{2+} obtained by ISCA1 reduced obviously with ISCA1 deficiency, which in further affected the Fe/S complex formation,

mitochondrial respiratory chain working and energy generation, finally leading to impaired iron regulation and occurrence of heart failure (HF) and multiple mitochondrial dysfunction syndromes type 5 (MMDS5).

Figures

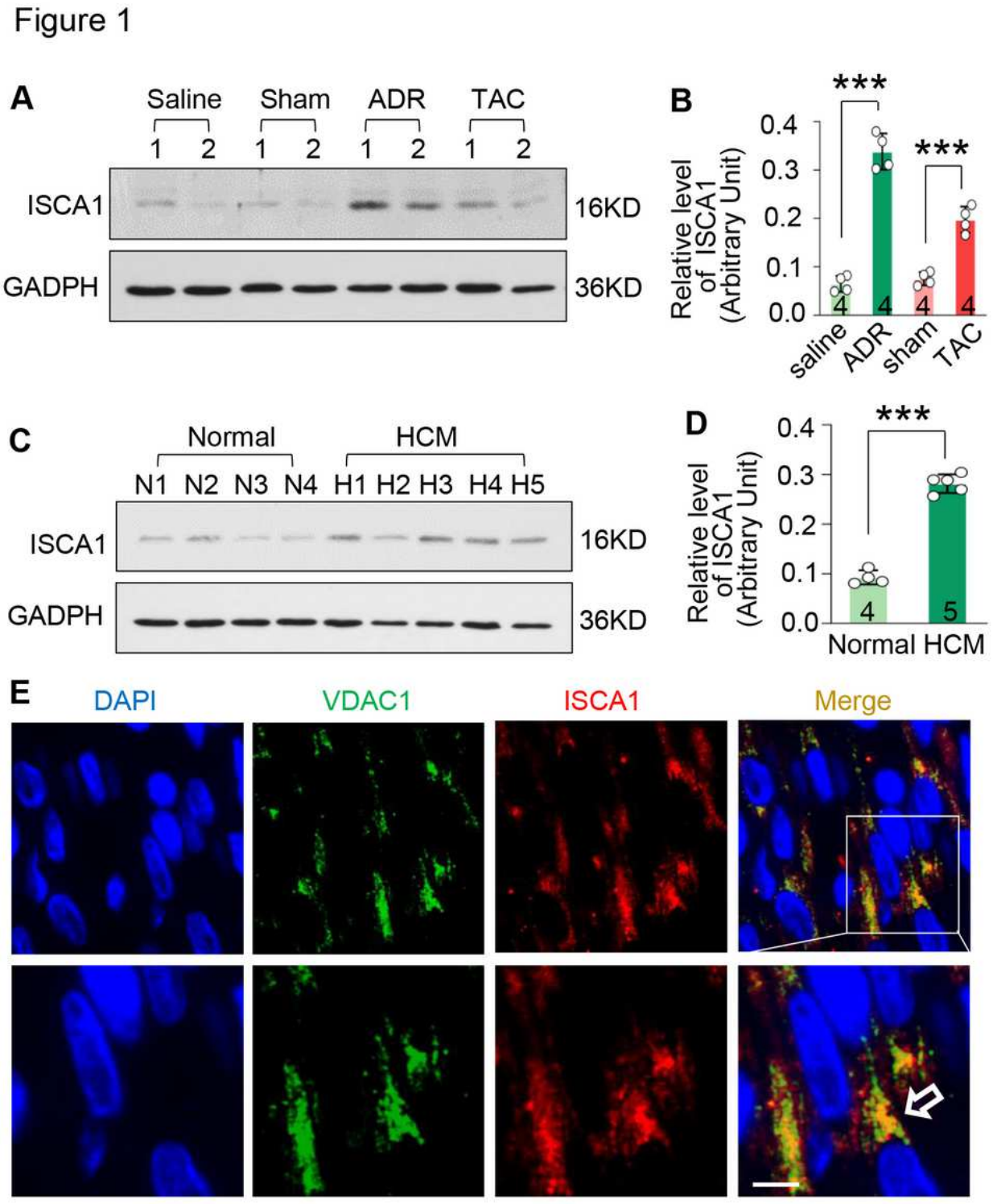

Figure 1

ISCA1 is induced under cardiomyopathy and heart failure and expressed in myocardial mitochondria. ISCA1 expression in heart tissues from adriamycin (ADR) treated and thoracic aorta constriction (TAC) mice models using GAPDH as normalization (A-B, n=4 mice per group, ***P<0.001 versus respective

control). ISCA1 expression in heart tissues from hypertrophic cardiomyopathy (HCM) patients and healthy heart donors using GAPDH as normalization (C-D, n=4 in normal and n=5 in HCM patients, ***P<0.001 versus normal). Immunofluorescence detection of ISCA1 and mitochondrial marker of VDAC1 in the heart tissues of WT rats at 2 weeks of age (E, n=4 rats per group, white scale bar = 5 μm).

Figure 2

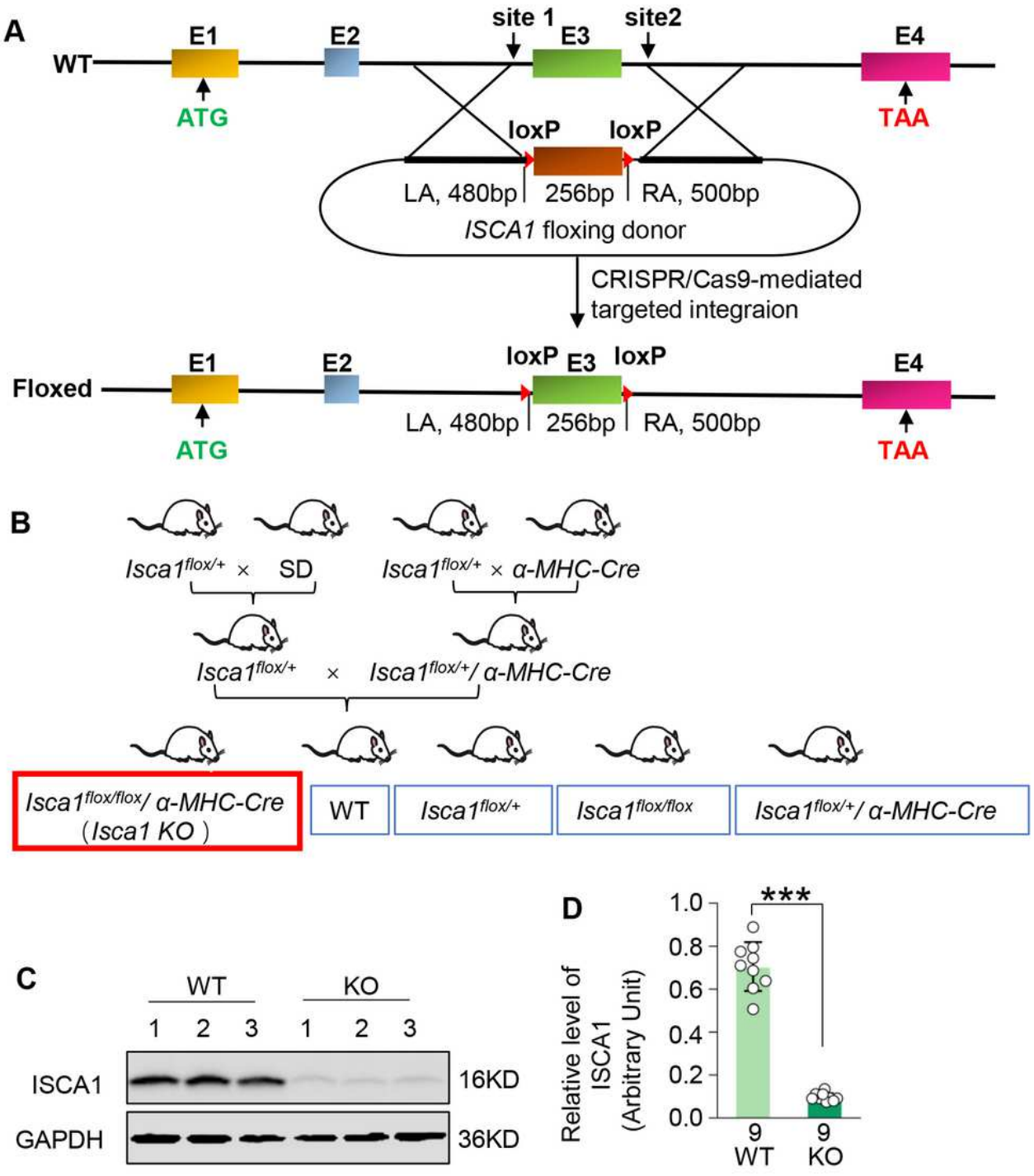

Figure 2

Establishment and identification for myocardial tissue specific knockout of Isca1 rat. Isca1 conditional knockout (Isca1 cKO) rats were generated by utilizing the Cre-loxP recombination system (A), which were then put two generation of cross mating with the α-MHC-Cre rats, and rats with myocardial tissue specific knockout of ISCA1 were obtained, referred as Isca1-KO (Isca1flox/flox/α-MHC-Cre) (B). The ISCA1 expression (C) in heart tissues from KO rat was detected using western blot (C-D, n = 9 rats per group, ***P<0.001 versus WT; LA: left arm, RA: right arm).

Figure 3

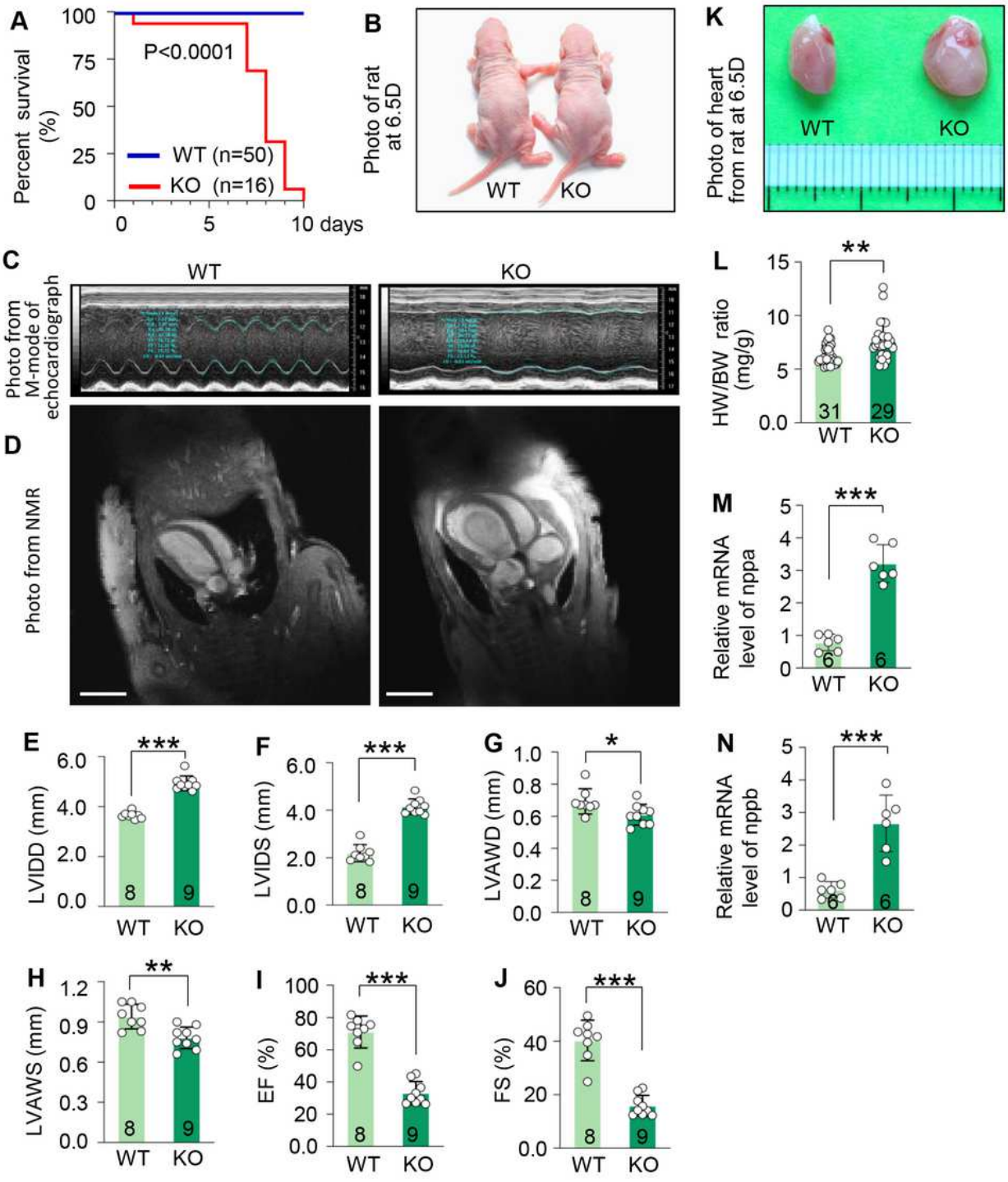

Figure 3

Myocardial specific ISCA1 deficiency induces severe HF in rats. Cumulative percent survival rate for WT (n=50) and KO (n=16) groups were calculated from 0 to 10 days after birth (A). Photographs of rats from WT and KO groups at 6.5 days of age (B). The M-mode echocardiography screenshot (C) and nuclear magnetic resonance (NMR) screenshot (D, white scale bar = 5 mm) from WT and KO groups at 6.5 days of age. Echocardiographic parameters of LVIDD, LVIDS, LVAWD, LVAWS, EF, and FS were analyzed in rats from both groups at 6.5 days of age (E-J, n=8 in WT group and n=9 in KO group, *P < 0.05, **P< 0.01, ***P<0.001 versus WT). Photograph of heart after dissection in rat from both groups at 6.5 days of age (K) and the heart weight to body weight (HW/BW) ratio was calculated (L, n=31 in WT group and n=29 in KO group, **P<0.01 versus WT). Quantitative analysis of nppa and nppb mRNA levels in myocardium from rats in both groups at 6.5 days of age by real-time PCR (M-N, n=6 rats per group, ***P<0.001 versus WT).

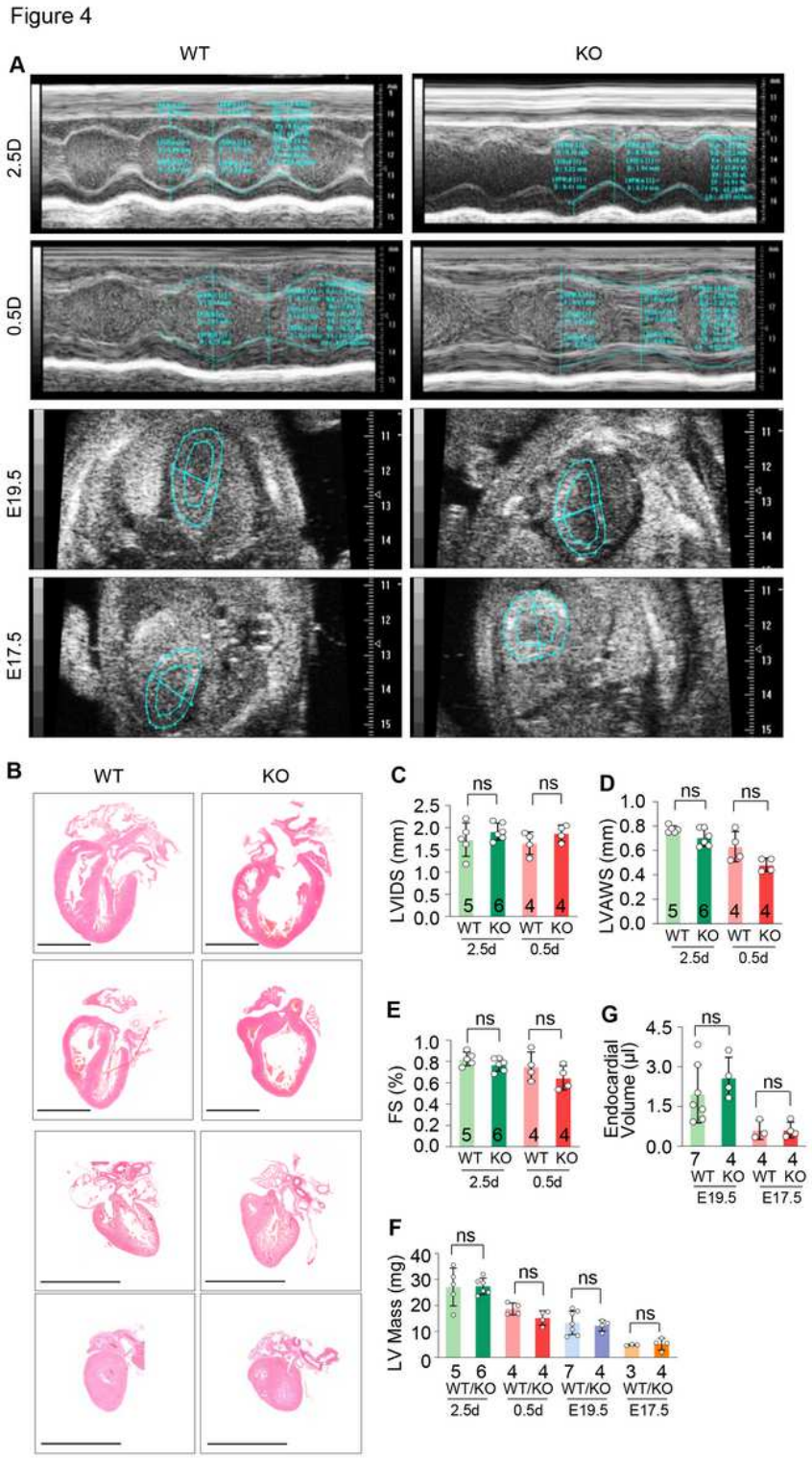

Figure 4

Trace the starting point of morphological differences. The M-mode echocardiography screenshot in both groups at 0.5 and 2.5 days after birth, and in the embryonic period of E17.5 and E19.5 (A). Representative photographs of the whole-heart longitudinal sections with H&E staining from both groups (B, black bar=2 mm). Echocardiographic parameters of LVIDS, LVAWS, FS, LV Mass, and endocardial volume were analyzed in rat from both groups at 6.5 days of age (C-G, ns: not significant).

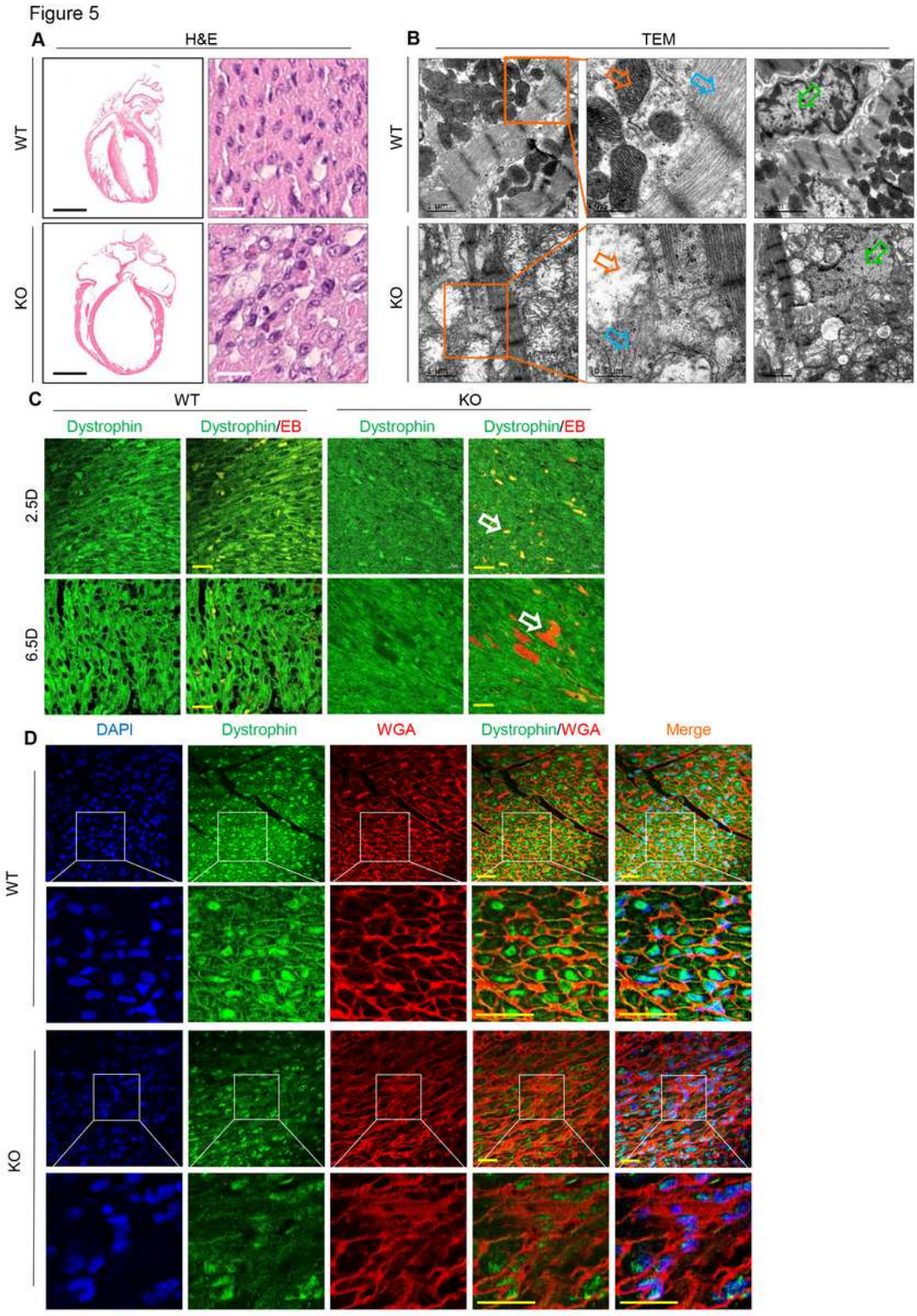

Figure 5

ISCA1 deficiency induces oncosis in myocardium. Representative photographs of the whole-heart longitudinal sections and its magnification with H&E staining from rats of WT and KO groups at 6.5 days of age (A, n = 4 rats per group, black bar=2 mm, white bar= 20 μm). Transmission electron microscope (TEM) analysis of left ventricular free walls from rats of WT and KO groups at 6.5 days of age (B, n = 4 rats per group, open orange arrow: mitochondria, open blue arrow: sarcomere, open green arrow: nuclear).

Representative photographs of immunofluorescence staining for dystrophin and Evans blue (EB) (C, n = 3 rats in WT group and n = 3 rats in KO group at 2.5 days of age, n = 4 rats in WT group and n = 3 rats in KO group at 6.5 days of age, yellow bar=20 μm, open white arrow: EB stain positive area). Representative photographs of immunofluorescence staining for dystrophin and wheat germ agglutinin (WGA) (D, n = 4 rats in WT group, n = 3 rats in KO group, yellow bar=20 μm).

Figure 6

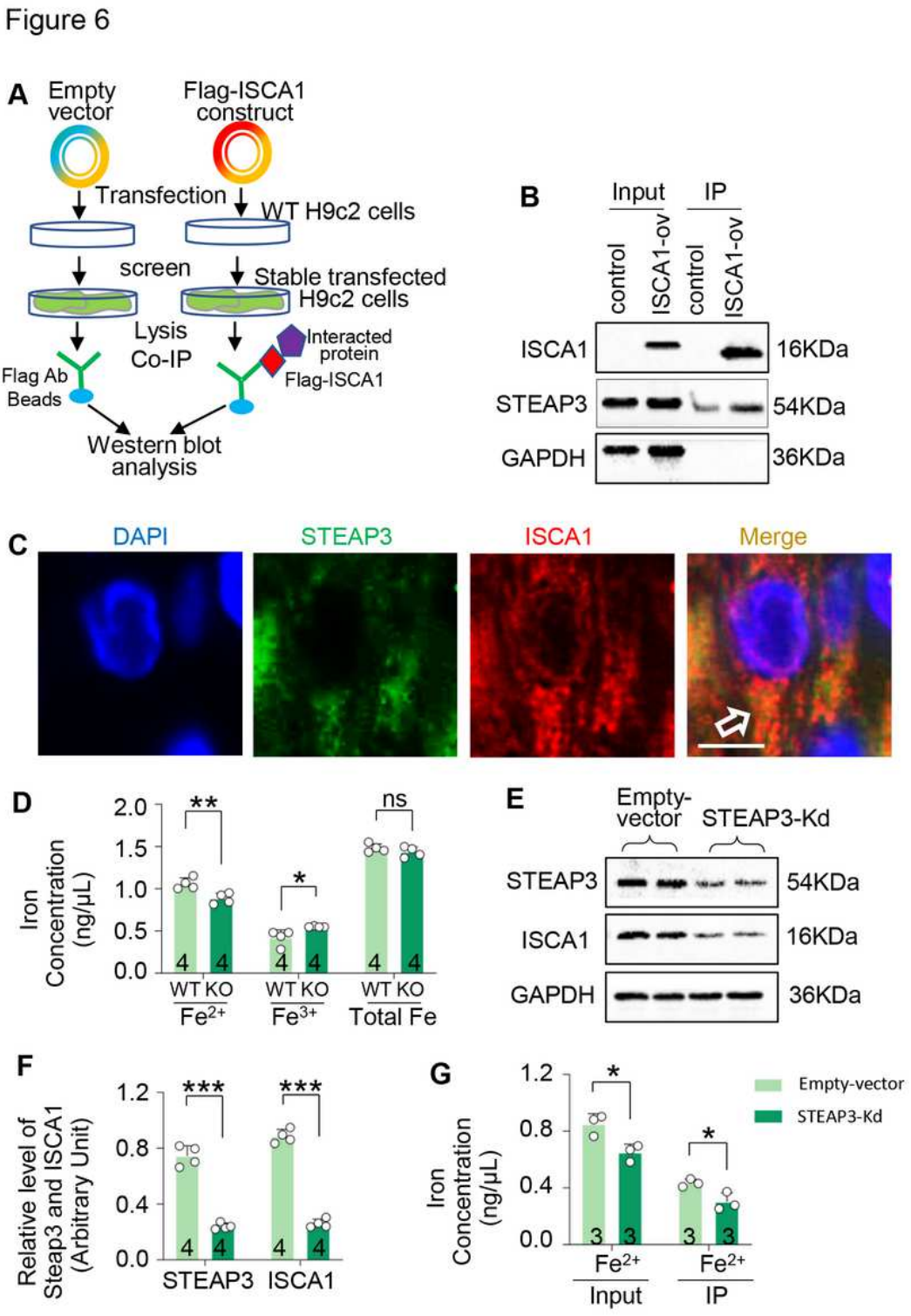

Figure 6

ISCA1 deficiency disrupts iron homeostasis in myocardium Screening processes for finding interacting molecules with ISCA1 using co-immunoprecipitation (Co-IP) and western blot analysis (A). Western blot verification for six-transmembrane epithelial antigen of prostate 3 (STEAP3), a molecule interacting with ISCA1 (B). Representative photographs of immunofluorescence staining for ISCA1 and STEAP3 in myocardium sections from wt rat at 6.5 days of age (C, n = 3 rats per group, white bar=5 μm). The total iron, ferrous iron (Fe^{2+}) and ferric iron (Fe^{3+}) levels in heart tissues of WT and KO rats were detected by colorimetry (D, n = 4 rats per group, *P < 0.05, **P< 0.01, versus WT group). The expression of STEAP3 and ISCA1 in empty-vector stably H9c2 cells and STEAP3-Kd stably H9c2 cells were detected using western blot (E). Quantitative analysis of ISCA1 and STEAP3 expression using GAPDH for normalization (F, n = 4 rats per group, ***P< 0.001, versus empty-vector group). The Fe^{2+} levels in both stably cells of empty-vector and STEAP3-Kd groups were detected by colorimetry after stimulation by ferric ammonium citrate (100 μM) in immunoprecipitation product pulled down by ISCA1 antibody (G) (*P<0.05, versus empty-vector group).

Figure 7

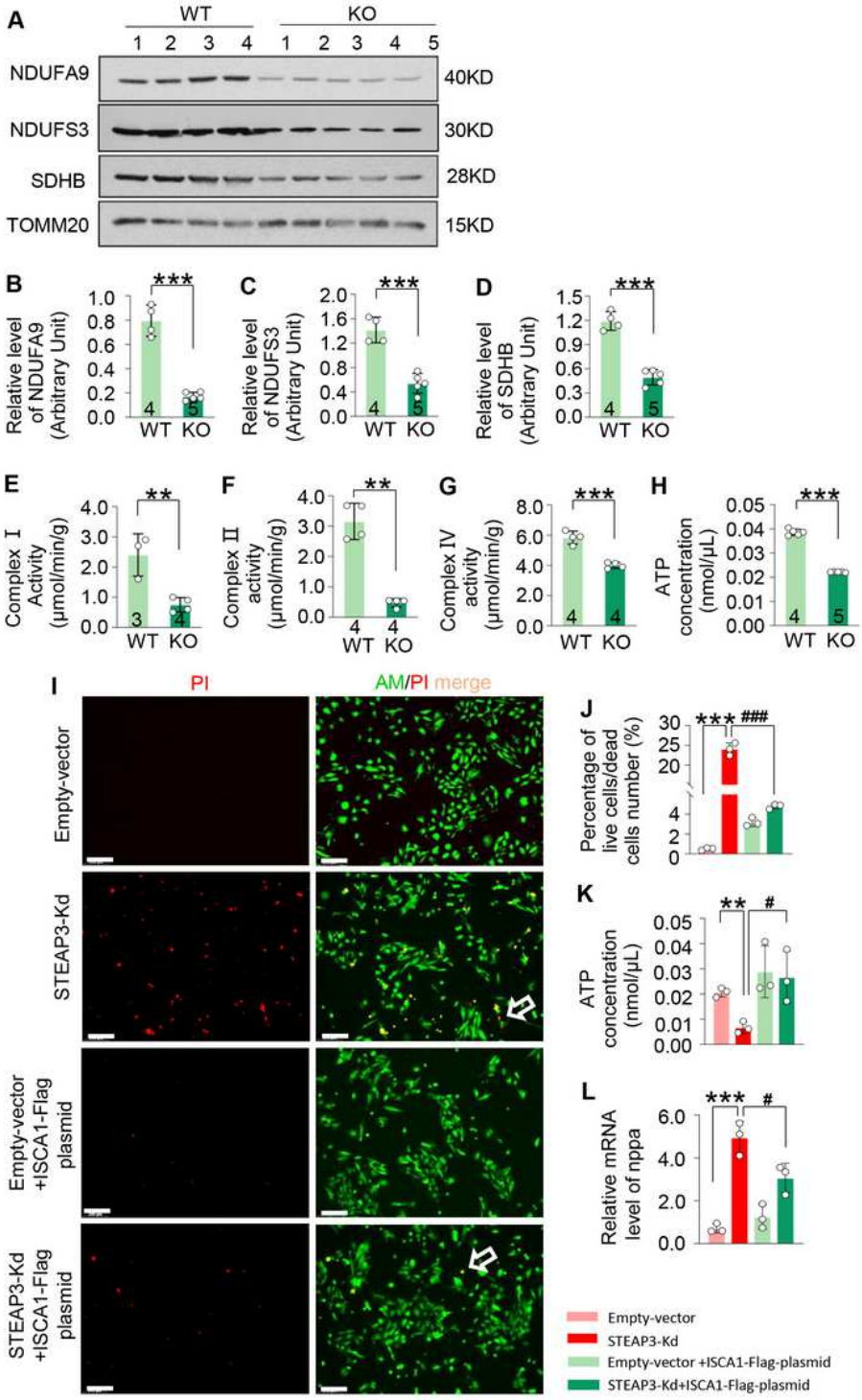

Figure 7

ISCA1 plays an important role in energy metabolism of myocardial mitochondrial respiratory chain. The expression level of NDUFA9 and NDUFS3 and SDHB were detected in myocardium from KO rats at 6.5 days of age through western blot (A). Quantitative analysis of NDUFA9, NDUFS3 and SDHB expression using TOMM20 for normalization (B-D, n=4 in WT group and n=5 in KO group□***P<0.001, versus WT group). The enzyme activity of complex □, □ and □ were detected in myocardium from KO rats using

colorimetric method (E-G, **P<0.01, ***P<0.001, versus WT group). The ATP generation in myocardial tissue from KO rat at 6.5 days of age was determined by colorimetry (H, n=4 in WT group and n=5 in KO group, ***P<0.001, versus WT group). Representative images of calcein AM/propidium iodide (PI) double staining in H9c2 cells of four group (I, empty-vector: stable empty-vector cells; STEAP3-Kd: stable STEAP3-Kd cells; empty-vector+ISCA1-Flag-plasmid: ISCA1-Flag plasmid was transient transfected to stable empty-vector cells; STEAP3-Kd+ISCA1-Flag-plasmid: ISCA1-Flag plasmid was transient transfected to stable STEAP3-Kd cells). Percentage of live cells/dead cells number after calcein AM/propidium iodide (PI) double staining (J, repeated assay three times independently, ***P<0.001, STEAP3-Kd group versus empty-vector group, ###P<0.001, STEAP3-Kd+ISCA1-Flag-plasmid group versus STEAP3-Kd group). The ATP generation in H9c2 cells of four groups were determined by colorimetry (K, repeated assay three times independently, **P<0.01, STEAP3-Kd group versus empty-vector group, #P<0.05, STEAP3-Kd+ISCA1-Flag-plasmid group versus STEAP3-Kd group). Quantitative analysis of nppa at mRNA levels in H9c2 cells from four groups were assayed by real-time PCR (L, repeated assay three times independently, ***P<0.001, STEAP3-Kd group versus empty-vector group, #P<0.05, STEAP3-Kd+ISCA1-Flag-plasmid group versus STEAP3-Kd group).

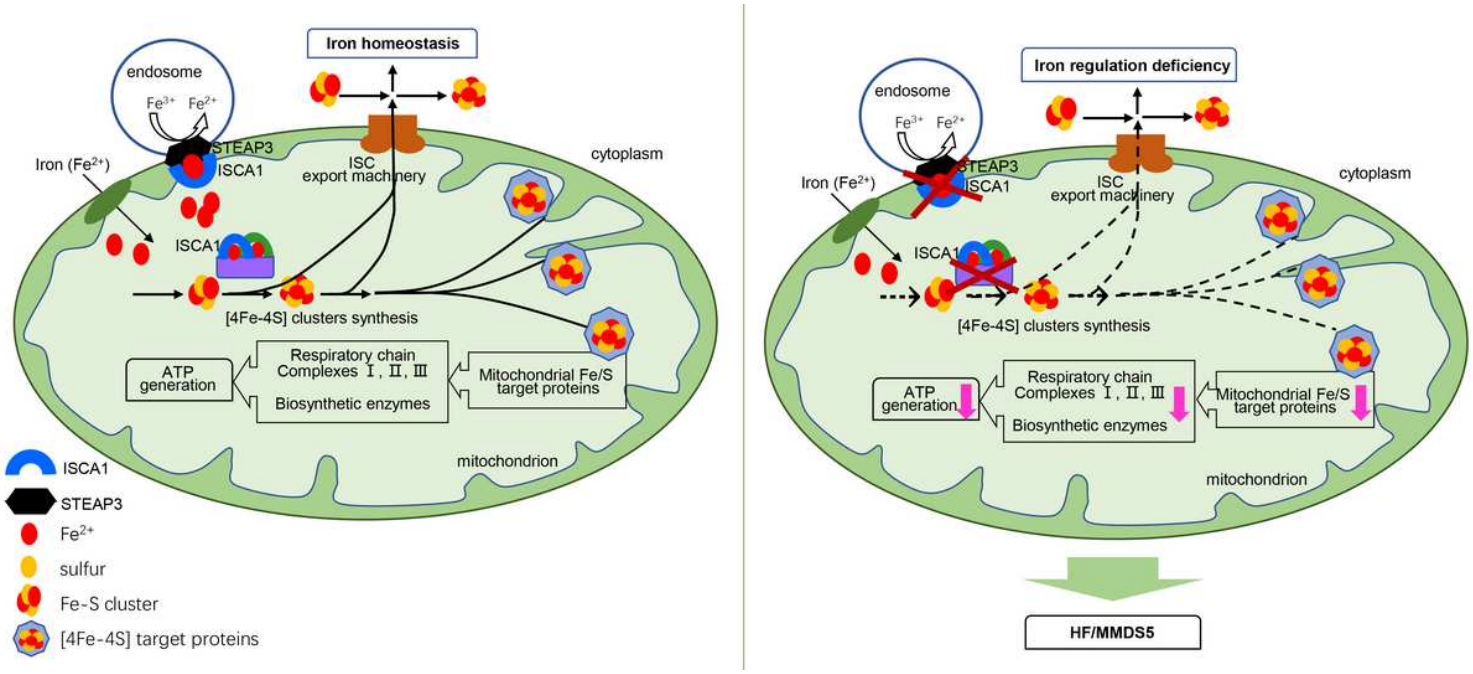

Figure 8

Schematic illustrating the alteration of iron metabolism in cytoplasm and mitochondrial due to the deficiency of ISCA1 in myocardium of KO rat. ISCA1 performed important role in maturation of mitochondrial [4Fe-4S] proteins in previous reports, thus, providing the basic assembly element for the formation of cytoplasm and mitochondrial Fe/S complex. We found that ISCA1 interacts with STEAP3 (Six-Transmembrane Epithelial Antigen of Prostate 3, functions as an iron transporter and reduce Fe3+ cation as a metalloreductase), and Fe2+ obtained by ISCA1 reduced significantly with STEAP3 knowdown regulated. Meanwhile, we found that the level of Fe3+ and Fe2+ undergo different degrees of regulation, and the iron homeostasis suffered a destruction in myocardium with ISCA1 deficiency. The

experimental results above suggested us that the interaction between ISCA1 and STEAP3 was seriously affected in the “Kiss and Run” mechanism (one of the five main mechanisms for transporting iron into the mitochondria) and Fe2+ obtained by ISCA1 reduced obviously with ISCA1 deficiency, which in further affected the Fe/S complex formation, mitochondrial respiratory chain working and energy generation, finally leading to impaired iron regulation and occurrence of heart failure (HF) and multiple mitochondrial dysfunction syndromes type 5 (MMDS5).

Supplementary Files

This is a list of supplementary files associated with this preprint. Click to download.

- onlinedatasupplements.docx
- keymessages.docx